TABLE 1. Patients' Characteristics

	Total	Year of Sampling				
		2008	2009	2010	2011	2012
Patients, n	1406	298	250	294	297	267
Male gender, n (%)	881 (62.7)	213 (71.5)	150 (60)	184 (62.6)	154 (51.9)	180 (67.4)
Age, median (range)	30 (16–66)	29 (16–58)	29 (20–60)	30 (17–55)	31 (19–66)	33 (18–65)
Living in HCMC, n (%)	735 (52.3)	163 (54.7)	132 (52.8)	148 (50.3)	150 (50.5)	142 (53.2)
Time since HIV diagnosis, n (%)						
<6 mo	975 (69.3	224 (75.2)	181 (72.4)	233 (79.3)	138 (46.5)	199 (74.5)
≥6 mo	431 (30.7)	74 (24.8)	69 (27.6)	61 (20.7)	159 (53.5)	68 (25.5)
Risk of HIV transmission, n (%)						
Heterosexual contact, alone	854 (60.7)	148 (49.7)	143 (57.2)	149 (50.7)	210 (70.7)	204 (76.4)
IDU, alone	315 (22.4)	73 (24.5)	68 (27.2)	90 (30.6)	44 (14.8)	40 (15.0)
Heterosexual and IDU	73 (5.2)	29 (9.7)	5 (2)	3 (1)	29 (9.8)	7 (2.6)
Homosexual contact	2 (0.1)	2 (0.7)	0	0	0	0
Other/unknown	162 (11.5)	46 (15.4)	34 (13.6)	52 (17.7)	14 (4.7)	16 (6.0)
HIV-1 subtype, n (%)						
CRF01_AE	1378 (98.0)	295 (99.0)	246 (98.4)	289 (98.3)	289 (97.3)	255 (95.5)
Subtype B	19 (1.5)	1 (0.7)	4 (1.6)	2 (1)	6 (2)	6 (2.2)
Other/unclassified	9 (0.8)	0	0	2 (0.7)	1 (0.6)	6 (2.2)
HBs antigen positive, n (%)	217 (15.4)	42 (14.1)	43 (17.2)	49 (16.7)	47 (15.8)	36 (13.5)
Anti-HCV antibody positive, n (%)	557 (39.6)	148 (49.7)	106 (42.4)	117 (39.8)	105 (35.4)	81 (30.3)
CD4 cell count, cells/μL, median (range)	110 (1–1322)	70 (1–1042)	115 (1–753)	95 (1–1048)	253 (2–1322)	47 (1–1211)
Plasma HIV-1 RNA levels, log copies/mL, median (range)	5.01 (1.59–6.90)	4.81 (1.69–5.70)	4.38 (1.69–5.70)	5.23 (1.59–6.61)	5.02 (2.31–6.90)	5.38 (1.60–6.83)

HCMC, Ho Chi Minh City; CRF01_AE, circulating recombinant form01_AE; HBs antigen, hepatitis B virus surface antigen; anti-HCV antibody, anti-hepatitis C virus antibody.

The presence of TDR did not correlate with any specific demographic factor, risk group, or year of study enrollment, although the odds ratio of acquiring TDR was relatively low in heterosexual individuals (Table 3). Annual trends of TDR prevalence in particular HIV risk categories are shown in Table 4. TDR prevalence in heterosexual contact alone, IDU alone, and IDU plus heterosexual contact were 3.33%, 5.41%, and 2.78% respectively, which were not statistically different. Although no significant annual trend was noted over the study period among them, the TDR prevalence in the HIV risk group of IDU alone were higher than the WHO first threshold 5% in the year 2009, 2010, and 2012 (4.10% in 2008, 5.88% in 2009, 6.67% in 2010, 2.27% in 2011%, and 7.69% in 2012). Phylogenetic tree analysis showed no clustering of sequences from the study participants with TDR. Details of the 4 individuals with TDR in more than 1 group of antiretrovirals are listed in Table 5. One individual had very extensive resistance: M41L, M184V, T215Y in NRTI-associated mutations, and Y181C and G190A in NNRTI-associated mutations. Overall, persistently low prevalence of TDR during the last 5 years of ART expansion was noted. However, individuals with multiple-drug resistances were identified during ART expansion. This finding highlights the importance of TDR and undermines the efficacy of currently scaled up ART regimens.

DISCUSSION

In this study, we traced the prevalence of TDR over a relatively long period of time (from 2008 to 2012) in treatment-naive individuals in Southern Vietnam during rapid ART scaling up program. Our result of 4.18% of overall TDR prevalence was similar to those described previously in Vietnam.[10–17] However, the study covered longer period of time and demonstrated the stability of TDR prevalence over this period. In comparison, all the other previous surveillance studies conducted in Vietnam were shorter in duration. Primary HIV drug resistance is one of the main concerns in any ART program because it can compromise the clinical outcome of ART, especially in countries with limited ART options. Our data of persistently low prevalence of TDR in Southern Vietnam possibly reflect the success of the recent ART scale-up program in this country.

The TDR rate in our study, however, ranged from 2.4% to 5.5%, reaching the threshold of low prevalence according to the WHO definition (<5%) in 2009, 2010, and 2012.[4] Considering lower viral replication fitness of strains harboring drug resistance mutations than that of wild-type strain, the rate of pretreatment resistance in chronic HIV infection could underestimate the real drug resistance transmission with time since HIV infection. In particular, the low-level prevalence of M184V[22] despite widespread use of lamivudine, which is sometimes used for treatment of hepatitis B virus infection, could be related to the lower viral fitness. Of note, the percentage of individuals diagnosed as HIV positive more than 6 months before study enrollment was higher in 2011 (53.5%) than that in other study periods, and the TDR prevalence in 2011 was lower (2.72%) than that in 2009, 2010, and 2012. Most cases had chronic HIV infection at the time of HIV

TABLE 2. Prevalence of Transmitted Drug Resistance Mutations

	Total	2008	2009	2010	2011	2012
Study population (n)	1389	292	250	292	294	261
Any TDR [n (%)]	58 (4.18)	7 (2.40)	13 (5.20)	16 (5.48)	8 (2.72)	14 (5.36)
RT in total [n (%)]	43 (3.10)	7 (2.40)	9 (3.60)	14 (4.79)	4 (1.36)	10 (3.83)
NRTI [n (%)]						
Any	28 (2.02)	3 (1.03)	6 (2.40)	11 (3.76)	3 (1.02)	5 (1.92)
Thymidine analog mutations						
M41L	2 (0.14)			1	1	
D67N	1 (0.07)		1			
D67E	1 (0.07)			1		
K70E	1 (0.07)			1		
T215Y	1 (0.07)				1	
T215I	1 (0.07)		1			
T215S	1 (0.07)				1	
T215D	2 (0.14)		2			
K219Q	3 (0.22)		1	2		
Others						
K65R	2 (0.14)			2		
L74V	1 (0.07)	1				
L74I	4 (0.29)	1		2		1
V75M	6 (0.43)	1		2		3
M184V	3 (0.22)		1		2	
M184I	2 (0.14)			1		1
NNRTI [n (%)]						
Any	19 (1.37)	5 (1.71)	3 (1.20)	4 (1.37)	3 (1.02)	4 (1.53)
K101E	4 (0.29)	1	2	1		
K103N	7 (0.50)	1	1	1		4
Y181C	6 (0.43)	1		2	1	2
Y188L	1 (0.07)				1	
Y188H	1 (0.07)			1		
Y188C	1 (0.07)			1		
G190A	4 (0.29)	2		1	1	
G190E	1 (0.07)				1	
PI [n (%)]						
Any	15 (1.08)	0	4 (1.60)	2 (0.68)	4 (1.36)	5 (1.92)
D30N	1 (0.07)				1	
M46I	4 (0.29)		2			2
M46L	6 (0.43)		1		3	2
M46I/L	1 (0.07)			1		
F53Y	1 (0.07)			1		
L76V	1 (0.07)					1
L90M	1 (0.07)		1			

diagnosis, and the exact latency from infection to diagnosis or to study enrollment was unavailable. Thus, the longer duration from diagnosis to study participation allows more frequent reversion from TDR into wild-type virus. This should be taken into account in the interpretation of the results of the study.

Although our study participants did not represent the national HIV-infected population in Vietnam but were rather HIV-infected individuals living in or near Ho Chi Minh City (HCMC), their age, sex, and the distribution of HIV risks were almost comparable with the national HIV-infected population in Vietnam. Notably, HCMC accounts for approximately 50% of the entire population receiving ART in Vietna,[12] and ART had been widely accessible in HCMC since the early phase of ART scale-up or even before ART scale-up at private clinics. Since previous studies had predicted increased TDR rates after 5–8 years of ART scale-up,[2] HIV-infected individuals in HCMC are considered to be at higher risk of TDR compared with those in other areas of Vietnam. In addition, a previous study conducted in HCMC showed that 73% of patients on ART reported having injected drugs,[1] and the sentinel surveillance in 2009 showed that HCMC had high HIV prevalence among IDUs (46%).[1] Since IDU is considered a risk factor for poor adherence and emergence of drug resistance,[23,24] patients in HCMC are considered the key population for TDR monitoring. Although no statistical relationship was

TABLE 3. Relation Between Demographic and Clinical Factors and the Presence of Transmitted Drug Resistance

	With TDR (n = 58)	Without TDR (n = 1331)	Odds Ratio*	95% CI	*P* Value
Male gender, n (%)	42	831	1.58	0.88 to 2.53	0.13
Age (yrs), n (%)					
<30	24	538	1.00		
30–39	22	557	0.98	0.54 to 1.78	0.95
≥40	12	178	1.67	0.82 to 3.42	0.16
Time since HIV diagnosis, n (%)					
<6 mo	46	923	1.00		
≥6 mo	12	401	0.60	0.31 to 1.15	0.12
Unknown	0	7			
Year of HIV diagnosis					
Before 2008	2	132	1.00		
2008	6	223	1.78	0.35 to 8.93	0.49
2009	13	301	2.85	0.63 to 12.8	0.17
2010	17	293	3.83	0.87 to 16.8	0.08
2011	8	149	3.54	0.74 to 17.0	0.11
2012	12	226	3.50	0.77 to 15.9	0.10
Unknown	0	7			
Year of study enrollment, n (%)					
2008	7	285	1.00		
2009	13	237	2.23	0.88 to 5.69	0.09
2010	16	276	2.36	0.96 to 5.83	0.06
2011	8	286	1.14	0.40 to 3.18	0.80
2012	14	247	2.31	0.92 to 5.81	0.08
Risk of HIV transmission, n (%)					
Heterosexual contact	30	883	0.60	0.33 to 1.09	0.05
Injection drug use	19	367	1.49	0.82 to 2.69	0.19
Other	1	20	1.19	0.16 to 9.07	0.86
Unknown	10	131			
HBs antigen positive, n (%)	12	205	1.43	0.74 to 2.74	0.28
HCV antibody positive, n (%)	19	533	0.72	0.41 to 1.27	0.26
CD4 cell count, cells/μl					
≥100	24	686	1.00		
<100	34	642	1.51	0.89 to 2.58	0.14
Unavailable	0	3			

*Logistic regression model was used for calculating odds ratio.
CI, confidence interval.

found in our study between TDR and various risk factors, the odds ratio was lowest for heterosexual contact, with a marginal *P* value of 0.05, which indirectly suggests that other risk groups, such as IDU or men who have sex with men, is at higher risk of TDR. Meanwhile, the proportion of IDUs in our study had decreased during the 5 years along with the nationwide shift from the concentrated HIV epidemic in male IDUs to the general population. Although we failed to find the statistical impact of HIV risk group on TDR prevalence, TDR prevalence among IDU were

TABLE 4. Prevalence of Transmitted Drug Resistance Mutations in Specific HIV Risk Categories

	Total	2008	2009	2010	2011	2012
Total TDR rate [% (n/total)]	4.18 (58/1389)	2.40 (7/292)	5.20 (13/250)	5.48 (16/292)	2.72 (8/294)	5.36 (14/261)
TDR rate in HIV risk categories [% (n/total)]						
Heterosexual contact alone	3.33 (28/840)	1.40 (2/143)	4.90 (7/143)	3.40 (5/147)	1.92 (4/208)	5.02 (10/199)
IDU alone	5.41 (17/314)	4.10 (3/73)	5.88 (4/68)	6.67 (6/90)	2.27 (1/44)	7.69 (3/39)
IDU plus heterosexual	2.78 (2/72)	3.45 (1/29)	0 (0/5)	0 (0/3)	3.57 (1/28)	0 (0/7)
Homosexual contact alone	0 (0/2)	0 (0/2)	- (0/0)	- (0/0)	- (0/0)	- (0/0)
Other	0 (0/20)	0 (0/13)	0 (0/3)	0 (0/1)	0 (0/3)	- (0/0)
Unknown	7.80 (11/141)	3.13 (1/32)	6.45 (2/31)	9.80 (5/51)	18.2 (2/11)	6.25 (1/16)

TABLE 5. Characteristics of 4 Patients With Drug Resistance Mutations Against Multiple Class Antiretrovirals

Patient ID	Year of HIV Diagnosis	Year of Study Participant	Sex	Risk of HIV Infection	CD4 Count (Cells/μL)	HIV-RNA (Log Copies/mL)	HBs Antigen	HCV Antibody	Resistance Mutations	
									NRTI	NNRTI
08HT0059	2003	2008	M	Heterosexual	10	4.11	Negative	Negative	L74V	V106I, G190A
10HT0136	2010	2010	F	Unknown	283	4.60	Negative	Negative	D67E	Y188C
11HT0201	2011	2011	F	Heterosexual	272	5.98	Positive	Negative	M41L, M184V, T215Y	Y181C, G190A
11HT0299	2011	2011	M	Unknown	147	5.83	Negative	Negative	M184V	V106I, V179D, Y188L

relatively higher, which was above 5% in 2009, 2010, and 2012 and had changed along with the overall TDR prevalence. These findings support that IDU is still important as a TDR risk factor in this population. In this regard, however, our study enrolled 141 patients who were free of possible HIV risk or refused to provide information on their risky behavior. Because their TDR prevalence was high over the study period, their concealment of IDU experience could influence the analysis. Although our study was conducted only in urban area, our findings in individuals at most risk of TDR are useful for the assessment of the situation in the near future of the entire HIV population in Vietnam, including rural area where ART has been rapidly distributed in recent years.

With respect to the drug class, the TDR prevalence was 2.02% for NRTI, 1.37% for NNRTI, and 1.08% for PI. Compared with the TDR rate for CRF01_AE strain in the TDR lists for surveillance[18] (2.9% for NRTI, 0.5% for NNRTI, and 1.5% for PI), the TDR prevalence of NNRTI-related mutations was higher for the entire study period and considered to have increased with ART scale-up. The Vietnamese national guideline for ART recommended nevirapine as one of the first-line regimen in 2005 and either nevirapine and efavirenz since 2009,[6–8] and generally NNRTI-base regimens have low genetic barriers for development of drug resistance. This background provides reasonable explanation of frequent detection of NNRTI-related mutations like in other resource-limited countries. However, TAMs and M184V or I were predominantly seen in NRTI-related mutations, which have clinically significant impact on treatment outcome. Even after changing the first-line NRTI in the national ART guideline from zidovudine (AZT) or stavudine (d4T) into tenofovir (TDF) in 2010, AZT or d4T were still extensively used in Vietnam over the study period. In Western Europe, a decline in the prevalence of TAMs is being observed in treatment-experienced cohort as a consequence of changing prescription patterns and prompt management of treatment failure.[25,26] Therefore, the TDR patterns in Vietnam could be changed with future increase in TDF use and decrease in AZT or d4T use. We should note that 4 individuals in our study had TDR in multiple drug classes, including 1 who had very extensive resistance: M41L, M184V, T215Y in NRTI and Y181C and G190A in NNRTI, which strongly compromise the efficacy of the first-line regimens in Vietnam and could threaten the nationwide ART scale-up program if it spreads. There are multiple factors that influence the prevalence of individual resistance mutations in primary HIV drug resistance but treatment-experienced persons with resistance might be the main source of such multiple-class TDR. Although continuous TDR surveillance is important to catch TDR expansion, efforts to enhance early diagnosis of treatment failure with improvement in availability of tests for plasma viral load and drug resistance in individuals on treatment, should be encouraged to prevent transmission of drug-resistant HIV.

In conclusion, TDR prevalence in Southern Vietnam remained low during the rapid scale-up of ART in 2008–2012. No demographic factor was statistically related to TDR detection, and the patterns of detected TDRs were similar to those described in previous reports. Although the average TDR prevalence was low, moderate prevalence was noted in part of the study period, and multiple-class TDR was detected in some patients. Because ART will continue to be scaled up, the TDR rate can rise in the future. Our results highlight the importance of TDR surveillance over a long period of time to provide proper assessment of the ART scale-up program.

ACKNOWLEDGMENTS

The authors thank Do Thi Cam Nhung for collecting the blood specimens, Keiko Saito, and Nguyen Thi Huyen for their assistance in study operation.

REFERENCES

1. National Committee for AIDS, Drug and Prostitution Prevention and Control, Ministry of Health, Socialist Republic of Viet Nam. *Viet Nam AIDS Response Progress Report 2012*. 2012. Available at: http://www.unaids.org/en/dataanalysis/knowyourresponse/countryprogressreports/2010countries/vietnam_2010_country_progress_report_en.pdf. Accessed September 30, 2013.
2. Gupta RK, Jordan MR, Sultan BJ, et al. Global trends in antiretroviral resistance in treatment-naive individuals with HIV after rollout of antiretroviral treatment in resource-limited settings: a global collaborative study and meta-regression analysis. *Lancet*. 2012;380:1250–1258.
3. Bennett DE, Bertagnolio S, Sutherland D, et al. The World Health Organization's global strategy for prevention and assessment of HIV drug resistance. *Antivir Ther*. 2008;13(suppl 2):1–13.
4. Jordan MR, Bennett DE, Wainberg MA, et al. Update on World Health Organization HIV drug resistance prevention and assessment strategy: 2004-2011. *Clin Infect Dis*. 2012;54:S245–S249.
5. Socialist Republic of Viet Nam. *Vietnam Country Progress Report 2010 on the Declaration of Commitment on HIV/AIDS, Adopted at the 26th United Nations General Assembly Special Session in 2001 (UNGASS)*. 2010. Available at: http://www.unaids.org/en/dataanalysis/knowyourresponse/countryprogressreports/2010countries/vietnam_2010_country_progress_report_en.pdf. Accessed September 30, 2013.
6. Ministry of Health, Socialist Republic of Viet Nam. *Antiretroviral Treatment Protocol for People Living With HIV/AIDS*. 2006 (No: 2051/QD-BYT).

7. Ministry of Health, Socialist Republic of Viet Nam. *Guidelines for Diagnosis and Treatment of HIV/AIDS*. 2009 (No. 3003/QĐ-BYT).
8. Ministry of Health, Socialist Republic of Viet Nam. *Guidelines for Diagnosis and Treatment of HIV/AIDS*. 2011 (No: 4139/QĐ-BYT).
9. The World Health Organization. *Consolidated Guidelines on the Use of Antiretroviral Drugs for Treating and Preventing HIV Infection: Recommendations for a Public Health Approach*. Geneva: WHO; 2013. Available at: http://www.who.about/licensing/copyright_form/en/index.html. Accessed September 30, 2013.
10. Lan NT, Recordon-Pinson P, Hung PV, et al. HIV type 1 isolates from 200 untreated individuals in Ho Chi Minh City (Vietnam): ANRS 1257 Study. Large predominance of CRF01_AE and presence of major resistance mutations to antiretroviral drugs. *AIDS Res Hum Retroviruses*. 2003;19:925–928.
11. Nguyen HT, Duc NB, Shrivastava R, et al. HIV drug resistance threshold survey using specimens from voluntary counseling and testing sites in Hanoi, Vietnam. *Antivir Ther*. 2008;13:115–121.
12. Duc NB, Hien BT, Wagar N, et al. Surveillance of transmitted HIV drug resistance using matched plasma and dried blood spot specimens from voluntary counseling and testing sites in Ho Chi Minh City, Vietnam, 2007-2008. *Clin Infect Dis*. 2012;54:S343–S347.
13. Tran VT, Ishizaki A, Nguyen CH, et al. No increase of drug-resistant HIV type 1 prevalence among drug-naive individuals in Northern Vietnam. *AIDS Res Hum Retroviruses*. 2012;28:1349–1351.
14. Dean J, Ta Thi TH, Dunford L, et al. Prevalence of HIV type 1 antiretroviral drug resistance mutations in Vietnam: a multicenter study. *AIDS Res Hum Retroviruses*. 2011;27:797–801.
15. Ayouba A, Lien TT, Nouhin J, et al. Low prevalence of HIV type 1 drug resistance mutations in untreated, recently infected patients from Burkina Faso, Côte d'Ivoire, Senegal, Thailand, and Vietnam: the ANRS 12134 study. *AIDS Res Hum Retroviruses*. 2009;25:1193–1196.
16. Bontell I, Cuong do D, Agneskog E, et al. Transmitted drug resistance and phylogenetic analysis of HIV CRF01_AE in Northern Vietnam. *Infect Genet Evo*. 2012;12:448–452.
17. Do TN, Nguyen TM, Do MH, et al. Combining cohort analysis and monitoring of HIV early-warning indicators of drug resistance to assess antiretroviral therapy services in Vietnam. *Clin Infect Dis*. 2012;54:S306–S312.
18. Bennett DE, Camacho RJ, Otelea D, et al. Drug resistance mutations for surveillance of transmitted HIV-1 drug-resistance: 2009 update. *PLoS One*. 2009;4:e4724.
19. Ariyoshi K, Matsuda M, Miura H, et al. Patterns of point mutations associated with antiretroviral drug treatment failure in CRF01_AE (subtype E) infection differ from subtype B infection. *J Acquir Immune Defic Syndr*. 2003;33:336–342.
20. Stanford HIV Drug Resistance Database. *Mutation Prevalence According to Subtype and Treatment*. Stanford, CA: Stanford University. Available at: http://hivdb.stanford.edu/cgi-bin/MutPrevBySubtypeRx.cgi. Accessed July 1, 2013.
21. Johnson VA, Calvez V, Gunthard HF, et al. Update of the drug resistance mutations in HIV-1: 2013. *Top Antivir Med*. 2013;21:6–14.
22. Paredes R, Sagar M, Marconi VC, et al. In vivo fitness cost of the M184V mutation in multidrug-resistant human immunodeficiency virus type 1 in the absence of lamivudine. *J Virol*. 2009;83:2038–2043.
23. Weber R, Huber M, Rickenbach M, et al. Uptake of and virological response to antiretroviral therapy among HIV-infected former and current injecting drug users and persons in an opiate substitution treatment programme: the Swiss HIV Cohort Study. *HIV Med*. 2009;10:407–416.
24. Werb D, Mills EJ, Montaner JS, et al. Risk of resistance to highly active antiretroviral therapy among HIV-positive injecting drug users: a meta-analysis. *Lancet Infect Dis*. 2010;10:464–469.
25. Cane P, Chrystie I, Dunn D, et al. UK Group on Transmitted HIV Drug Resistance. Time trends in primary resistance to HIV drugs in the United Kingdom: multicentre observational study. *Br Med J*. 2005;331:1368–1374.
26. Payne BA, Nsutebu EF, Hunter ER, et al. Low prevalence of transmitted antiretroviral drug resistance in a large UK HIV-1 cohort. *J Antimicrob Chemother*. 2008;62:464–468.

Low Raltegravir Concentration in Cerebrospinal Fluid in Patients With ABCG2 Genetic Variants

Kiyoto Tsuchiya, PhD, Tsunefusa Hayashida, PhD,* Akinobu Hamada, PhD,†‡ Shingo Kato, PhD,§ Shinichi Oka, MD, PhD,*‖ and Hiroyuki Gatanaga, MD, PhD*‖*

Abstract: Adenosine triphosphate–binding cassette transporter G2 (ABCG2) is expressed on the cerebrospinal fluid (CSF) side of choroid plexus epithelial cells, which form the blood–CSF barrier. Raltegravir was recently identified as a substrate of ABCG2. In the present study, we analyzed the relationship between single-nucleotide polymorphisms of ABCB1 and ABCG2 genes and raltegravir concentrations in 31 plasma and 14 CSF samples of HIV-infected patients treated with raltegravir-containing regimens. The mean CSF raltegravir concentration was significantly lower in CA (25.5 ng/mL) and AA (<10 ng/mL) genotypes at position 421 in ABCG2 gene compared with CC (103.6 ng/mL) genotype holders ($P = 0.016$).

Key Words: antiretroviral therapy, raltegravir, cerebrospinal fluid concentrations, blood–cerebrospinal fluid barrier, adenosine triphosphate–binding cassette transporter G2

(*J Acquir Immune Defic Syndr* 2014;66:484–486)

INTRODUCTION

Anatomical sanctuary sites in HIV-infected patients, where local drug exposure is lower than systemic compartment, are currently under intense investigation because they are suspected of hindering viral elimination by antiretroviral therapy (ART) and acting as sites for the selection of drug-resistant viruses during combination treatment. Especially the brain, the largest sanctuary site, in which residual viruses may cause chronic encephalitis and neurocognitive disorders, is one of the hottest foci of current HIV researches. Raltegravir, one of the preferred integrase inhibitors in the current ART guidelines, is highly effective in penetrating the central nervous system,[1] although a high interpatient variability has also been reported.[2,3]

Anatomically, the blood–cerebrospinal fluid (CSF) barrier makes tight junction and consists of choroid plexus epithelial cells in the cerebral ventricle. The adenosine triphosphate–binding cassette transporter B1 (ABCB1), also known as P-glycoprotein or multidrug resistance protein 1, and the adenosine triphosphate–binding cassette transporter G2 (ABCG2), also known as breast cancer resistance protein, are expressed on the CSF side of choroid plexus epithelial cells, and both are involved in the active transport of drugs.[4,5] Moreover, ABCB1 and ABCG2 are also expressed in the intestines and contribute to the absorption of the drugs. Recently, raltegravir was found to be a substrate of both ABCB1 and ABCG2.[6] In the present study, we analyzed the relations between raltegravir plasma and CSF concentrations and single-nucleotide polymorphisms (SNPs) of ABCB1 and ABCG2 genomes.

MATERIALS AND METHODS

HIV-1–infected patients treated with raltegravir-containing regimens (raltegravir 400 mg twice daily with 2 nucleotide/nucleoside reverse transcriptase inhibitors and/or protease inhibitors) were recruited at the AIDS Clinical Center, National Center for Global Health and Medicine, Tokyo, Japan. Blood samples were withdrawn into heparinized tubes 12 hours after raltegravir dosing (trough level), and the plasma was separated and stored at −80°C. Stocked residues of CSF samples taken 3–4 hours after raltegravir dosing for clinical purposes were also subjected to analysis. The Ethics Committee for Human Genome Studies at the National Center for Global Health and Medicine approved this study (NCGM-A-000122-02) and allowed us the use of only residues of samples that were originally obtained for clinical purposes. Each patient provided a written informed consent.

Plasma and CSF raltegravir concentrations were measured by the reverse-phase high-performance liquid chromatography (HPLC) method. Briefly, 200 μL of plasma or CSF and 400 μL of ethyl acetate were vortexed in a tube for 10 seconds and centrifuged. The organic phase was transferred to a new tube and evaporated to dryness. Subsequently, the

Received for publication January 16, 2014; accepted April 23, 2014.

From the *AIDS Clinical Center, National Center for Global Health and Medicine, Tokyo, Japan; †Department of Clinical Pharmacology, Group for Translational Research Support Core, National Cancer Center Research Institute, Tokyo, Japan; ‡Department of Medical Oncology and Translational Research, Kumamoto University, Kumamoto, Japan; §Department of Microbiology and Immunology, Keio University School of Medicine, Tokyo, Japan; and ‖Center for AIDS Research, Kumamoto University, Kumamoto, Japan.

Supported by The Grant for National Center for Global Health and Medicine (H22-110) and a Grant-in-Aid for AIDS Research from the Japanese Ministry of Health, Labour and Welfare (H23-AIDS-001).

S.O. has received honoraria and research grants from MSD, Janssen Pharmaceutical, Abbott, Roche Diagnostics, and Pfizer and also honoraria from ViiV Healthcare, Torii Pharmaceutical, Bristol-Myers, Astellas Pharmaceutical, GlaxoSmithKline, Taisho Toyama Pharmaceutical, Dainippon Sumitomo Pharma, and Daiichisankyo. H.G. has received honoraria from MSD, Janssen Pharmaceutical, Abbott, ViiV Healthcare, and Torii Pharmaceutical. The remaining authors have no conflicts of interest to disclose.

Correspondence to: Hiroyuki Gatanaga, MD, PhD, AIDS Clinical Center, National Center for Global Health and Medicine, 1-21-1 Toyama, Shinjuku-ku, Tokyo 162-8655, Japan (e-mail: higatana@acc.ncgm.go.jp).

residue was reconstituted in 250 μL of mobile phase, and 50 μL was injected into HPLC. Chromatography was performed, using Chromaster HPLC system (Hitachi, Tokyo, Japan) with RF-10A fluorescence detector (Shimadzu, Kyoto, Japan). Inertsil ODS-3 column (150 × 4.6 mm, 5-μm particle size; GL Sciences, Tokyo, Japan) was used as the analytical column. The flow rate was maintained at 1.5 mL per minute with fluorescence detection at 307 nm (excitation) and 415 nm (emission). The mobile phase consisted of acetonitrile/ethanol/phosphoric acid/water (20.8:20.8:0.1:58.3, vol/vol). Raltegravir calibration standards ranged from 10 to 2500 ng/mL. The accuracy of the analysis at 3 concentration levels ranged from −8.4% to +4.9%. Intraassay and interassay precisions were <4.8% and <7.6%, respectively. This assay was validated for both plasma and CSF raltegravir concentrations.

Genomic DNA was isolated from peripheral blood mononuclear cell, using a QIAamp DNA Mini Kit (Qiagen, Hilden, Germany). Genotyping of allelic variants of ABCB1 1236 C>T (rs1128503), 2677 G>T/A (rs2032582), 3435 C>T (rs1045642), 4036 A>G (rs3842), and ABCG2 421 C>A (rs2231142) was carried out using the TaqMan Drug Metabolism Assays by the ABI PRISM 7900HT sequence detection system (Applied Biosystems, Foster City, CA), according to the protocol provided by the manufacturer.

Differences between the groups were analyzed for statistical significance using the Kruskal–Wallis test. *P* values <0.05 denoted the presence of statistically significant difference. Analysis was performed using the SPSS Statistics software version 21 (IBM, Armonk, NY).

RESULTS

Plasma samples were collected from 31 patients, and stocked CSF samples from another group of 14 patients were used for the measurement of raltegravir concentrations.

All 45 patients (Japanese = 44, Myanmarian = 1) were subjected to SNP analysis of ABCB1 and ABCG2 genomes (Table 1). At position 1236 of ABCB1 gene, CC, CT, and TT genotypes were identified in 7, 21, and 17 patients, respectively. At position 2677, GG, GT, TT, GA, TA, and AA genotypes were identified in 8, 14, 11, 7, 4, and 1 patients, respectively. At position 3435, CC, CT, and TT genotypes were identified in 14, 17, and 14 patients, respectively. At position 4036, AA, AG, and GG genotypes were identified in 25, 18, and 2 patients, respectively. None of the genotypes of these SNPs in ABCB1 genome showed significant correlation with raltegravir concentration in plasma or CSF. At position 421 of ABCG2 gene, CC, CA, and AA genotypes were identified in 26, 14, and 5 patients, respectively. There was no significant correlation between the genotype at position 421 and trough concentration of raltegravir in plasma (Fig. 1A). However, in all 3 AA genotype holders, CSF raltegravir concentration was less than the lower limit of quantification (10 ng/mL) (Fig. 1B). Furthermore, in one of 4 CA genotype holders, CSF raltegravir concentration was below the detection limit, although it was higher than 25 ng/mL in any of the 7 CC genotype holders. The CA and AA genotype holders had significantly lower raltegravir concentrations in the CSF than the CC

TABLE 1. Genotype Frequencies of ABCB1 and ABCG2 Polymorphisms and Raltegravir Concentrations

		n	Raltegravir Concentration (ng/mL)*	*P*
Plasma (n = 31)				
ABCB1				
1236 C>T	rs1128503			
CC		3	480.1 ± 347.7	
CT		16	489.5 ± 602.4	0.485
TT		12	289.9 ± 324.5	
2677 G>T/A	rs2032582			
GG		5	254.6 ± 161.2	
GT		12	569.9 ± 716.6	
TT		6	197.1 ± 70.5	0.254
GA		4	648.9 ± 208.4	
TA		4	215.1 ± 219.4	
3435 C>T	rs1045642			
CC		9	358.2 ± 253.9	
CT		13	533.5 ± 659.0	0.680
TT		9	287.8 ± 362.0	
4036 A>G	rs3842			
AA		17	408.5 ± 535.7	
AG		13	402.5 ± 457.7	0.594
GG		1	572.8	
ABCG2				
421 C>A	rs2231142			
CC		19	355.5 ± 366.8	
CA		10	550.1 ± 699.0	0.779
AA		2	247.8 ± 88.7	
CSF (n = 14)				
ABCB1				
1236 C>T	rs1128503			
CC		4	140.8 ± 151.5	
CT		5	35.6 ± 19.5	0.330
TT		5	23.2 ± 14.7	
2677 G>T/A	rs2032582			
GG		3	31.7 ± 20.0	
GT		2	36.1 ± 23.6	
TT		5	23.2 ± 14.7	0.137
GA		3	188.0 ± 146.5	
AA		1	<10	
3435 C>T	rs1045642			
CC		5	122.5 ± 137.5	
CT		4	30.4 ± 18.6	0.325
TT		5	24.6 ± 17.5	
4036 A>G	rs3842			
AA		8	41.5 ± 56.6	
AG		5	103.0 ± 132.5	0.061
GG		1	<10	
ABCG2				
421 C>A	rs2231142			
CC		7	103.6 ± 116.0	
CA		4	25.5 ± 16.8	0.016
AA		3	<10	

*Data are mean ± SD for concentrations ≥10 ng/mL.

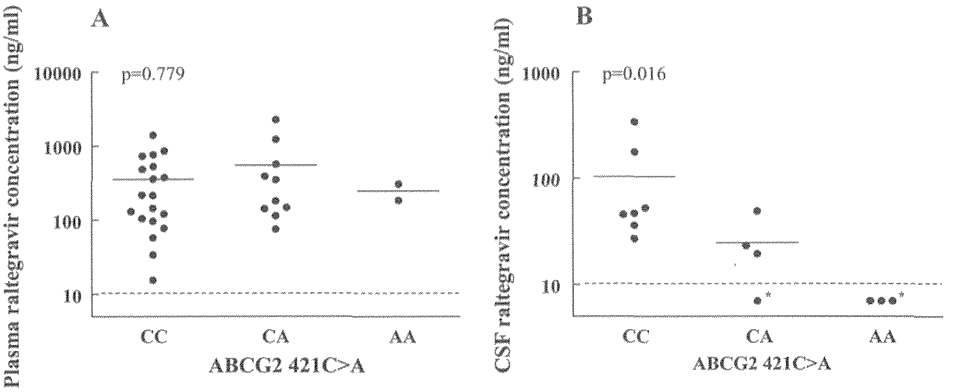

FIGURE 1. ABCG2 421C>A genotype and raltegravir concentration in plasma at trough level (A) and in CSF (B). Horizontal straight line indicates mean value; dashed line indicates the lower limit of quantification (10 ng/mL). *<10 ng/mL of raltegravir concentration.

genotype holders ($P = 0.016$), when the concentration below the lower limit of quantification was considered 10 ng/mL.

DISCUSSION

ABCG2 is diffusely expressed, whereas ABCB1 is weakly expressed on the CSF side of choroid plexus epithelial cells,[7,8] suggesting that the contribution of ABCB1 may be minor and that ABCG2 expression level in the choroid plexus is more likely to influence raltegravir concentration in the CSF than ABCB1. Previous studies indicated that genetic polymorphism of ABCG2 altered the protein expression level in plasmid transfection experiments.[9,10] Especially, C to A nucleotide substitution at position 421 significantly reduced the expression. The low expression induced by this nucleotide substitution may impair raltegravir transport from capillary blood to CSF, resulting in low raltegravir concentrations in CSF in holders of the CA/AA genotype at position 421. However, this SNP did not alter plasma raltegravir concentration significantly. Transporters other than ABCG2 may also exist in the intestines and further enhance raltegravir absorption. The presence of any antiretroviral at a concentration lower than that required for viral suppression could select drug-resistant HIV variants. In fact, we reported previously one patient with CSF raltegravir-resistant HIV variant, although the variant was not detected in the plasma.[11] The present study indicate that the genotype of this patient was AA at position 421 and that raltegravir concentration was below the lower limit of quantification in the CSF of this patient. Special attention should be paid to the raltegravir-containing ART of individuals with the CA/AA genotype at position 421 with active viral replication in the CNS, such as patients with HIV encephalitis.

Our study has certain limitations. Raltegravir concentrations were measured in plasma at trough level in 31 patients, and it was measured in stocked CSF samples of another group of 14 patients. First, we could not investigate the correlation between plasma and CSF concentrations because no paired plasma and CSF samples from the same subjects were available. Second, the time of CSF sampling in relation to raltegravir dosing varied among 3–4 hours. However, the population pharmacokinetic modeling of raltegravir concentration in the CSF showed a stable time course regardless of the dosing time.[2,12] Therefore, it is unlikely that the sampling time had a large impact on CSF concentration of the CA/AA genotype at position 421 in ABCG2 gene. Further analysis of the correlation between ABCG2 genotype and raltegravir CSF concentration is warranted.

ACKNOWLEDGMENTS

The authors thank Dr. Fumihide Kanaya for helping to prepare the manuscript. They also thank the clinical and laboratory staff of the AIDS Clinical Center, National Center for Global Health and Medicine, for the helpful support.

REFERENCES

1. Letendre S, Marquie-Beck J, Capparelli E, et al. Validation of the CNS penetration-effectiveness rank for quantifying antiretroviral penetration into the central nervous system. *Arch Neurol.* 2008;65:65–70.
2. Yilmaz A, Gisslén M, Spudich S, et al. Raltegravir cerebrospinal fluid concentrations in HIV-1 infection. *PLoS One.* 2009;4:6877.
3. Calcagno A, Cusato J, Simiele M, et al. High interpatient variability of raltegravir CSF concentrations in HIV-positive patients: a pharmacogenetic analysis. *J Antimicrob Chemother.* 2014;69:241–245.
4. Zhuang Y, Fraga CH, Hubbard KE, et al. Topotecan central nervous system penetration is altered by a tyrosine kinase inhibitor. *Cancer Res.* 2006;66:11305–11313.
5. Redzic Z. Molecular biology of the blood-brain and the blood-cerebrospinal fluid barriers: similarities and differences. *Fluids Barriers CNS.* 2011;8:3.
6. Hashiguchi Y, Hamada A, Shinohara T, et al. Role of P-glycoprotein in the efflux of raltegravir from human intestinal cells and CD4+ T-cells as an interaction target for anti-HIV agents. *Biochem Biophys Res Commun.* 2013;439:221–227.
7. Tachikawa M, Watanabe M, Hori S, et al. Distinct spatio-temporal expression of ABCA and ABCG transporters in the developing and adult mouse brain. *J Neurochem.* 2005;95:294–304.
8. Gazzin S, Strazielle N, Schmitt C, et al. Differential expression of the multidrug resistance-related proteins ABCb1 and ABCc1 between blood-brain interfaces. *J Comp Neurol.* 2008;510:497–507.
9. Imai Y, Nakane M, Kage K, et al. C421A polymorphism in the human breast cancer resistance protein gene is associated with low expression of Q141K protein and low-level drug resistance. *Mol Cancer Ther.* 2002;1:611–616.
10. Kondo C, Suzuki H, Itoda M, et al. Functional analysis of SNPs variants of BCRP/ABCG2. *Pharm Res.* 2004;21:1895–1903.
11. Watanabe K, Honda M, Watanabe T, et al. Emergence of raltegravir-resistant HIV-1 in the central nervous system. *Int J STD AIDS.* 2010;21:840–841.
12. Croteau D, Letendre S, Best BM, et al. Total raltegravir concentrations in cerebrospinal fluid exceed the 50-percent inhibitory concentration for wild-type HIV-1. *Antimicrob Agents Chemother.* 2010;54:5156–5160.

Superimposed Epitopes Restricted by the Same HLA Molecule Drive Distinct HIV-Specific CD8$^+$ T Cell Repertoires

Xiaoming Sun,*,[1] Mamoru Fujiwara,*,[1] Yi Shi,†,[1] Nozomi Kuse,* Hiroyuki Gatanaga,*,‡ Victor Appay,*,§ George F. Gao,† Shinichi Oka,*,‡ and Masafumi Takiguchi*

Superimposed epitopes, in which a shorter epitope is embedded within a longer one, can be presented by the same HLA class I molecule. CD8$^+$ CTL responses against such epitopes and the contribution of this phenomenon to immune control are poorly characterized. In this study, we examined HLA-A*24:02–restricted CTLs specific for the superimposed HIV Nef epitopes RYPLTFGWCF (RF10) and RYPLTFGW (RW8). Unexpectedly, RF10-specific and RW8-specific CTLs from HIV-1–infected HLA-A*24:02$^+$ individuals had no overlapping Ag reactivity or clonotypic compositions. Single-cell TCR sequence analyses demonstrated that RF10-specific T cells had a more diverse TCR repertoire than did RW8-specific T cells. Furthermore, RF10-specific CTLs presented a higher Ag sensitivity and HIV suppressive capacity compared with RW8-specific CTLs. Crystallographic analyses revealed important structural differences between RF10– and RW8–HLA-A*24:02 complexes as well, with featured and featureless conformations, respectively, providing an explanation for the induction of distinct T cell responses against these epitopes. The present study shows that a single viral sequence containing superimposed epitopes restricted by the same HLA molecule could elicit distinct CD8$^+$ T cell responses, therefore enhancing the control of HIV replication. This study also showed that a featured epitope (e.g., RF10) could drive the induction of T cells with high TCR diversity and affinity. *The Journal of Immunology*, **2014, 193: 77–84.**

Cytotoxic CD8$^+$ T lymphocytes recognize target cells through the recognition of peptides 8–11 aa long that are presented by MHC class I (MHCI) molecules (1–3). Of note, two epitopes in which a shorter one is embedded within a longer one are defined as superimposed epitopes, and they have been shown to be presented by the same MHCI molecule (4–6). A number of studies have reported CTL responses against such superimposed peptides in the context of an HIV-1 infection (7–10). For instance, these responses include CTLs specific for HLA-B57–restricted p24 Gag-derived peptides, for example, KI8 (residues 162–169, KAFSPEVI) and KF11 (residues 162–172, KAFSPEVIPMF), as well as for HLA-B*35:01–restricted Nef-derived peptides, for example, VY8 (residues 74–81, VPLRPMTY) and RY11 (residues 71–81, RPQVPLRPMTY). However, the biological relevance of this phenomenon remains unclear. Indeed, although it is speculated that CTLs can show cross-reactivity toward superimposed epitopes and work together effectively against HIV-infected targets, the functional synergism of these cells has not been studied in detail.

HLA-A*24:02 is the most frequent HLA class I allele in Japan, being found in ~70% of Japanese individuals (11) and of those infected with HIV-1 (12, 13). This allele also occurs in the range from ~25–64% in other Asian countries and in 18% in white populations (14, 15). Therefore, the study of immune responses to epitopes restricted by this allele is important for our understanding of HIV pathogenesis and vaccine development. We previously reported that Nef138-10 (RYPLTFGWCF, RF10) is an immunodominant CTL epitope in HLA-A*24:02$^+$ Japanese individuals chronically infected with HIV-1 (16, 17). Of interest, Nef138-8 (RYPLTFGW, RW8) is also defined as an optimal epitope presented by HLA-A*24:02 in white individuals (18). Although these superimposed epitopes elicit effective specific CTL responses important for the control of HIV-1 replication in HLA-A*24:02$^+$ individuals, the overlap in terms of reactivity and antiviral ability between RF10- and RW8-specific CTLs remains unknown.

In the present study, we performed a comprehensive analysis of CTL responses specific for RW8- and RF10-superimposed epitopes by using multiple approaches. We used RF10 and RW8 tetramers to identify and isolate cells from chronically HIV-1–infected HLA-A*24:02$^+$ Japanese individuals, α- and β-chain TCR repertoire analyses at the single-cell level to assess the degree of overlap between responses, and crystallographic approaches to reveal the structural basis of RF10– and RW8–HLA-A*24:02 interactions. We report unanticipated differences between RF10- and RW8-specific CTLs, that is, the elicitation of totally distinct CTL responses against superimposed HIV-1 epitopes restricted by the same HLA molecule, as well as distinct TCR repertoires between the featured (RF10) and featureless (RW8) epitope-specific CTLs.

Materials and Methods

Patient samples

The study was approved by the Ethics Committees of Kumamoto University and the National Center for Global Health and Medicine. Informed consent

*Center for AIDS Research, Kumamoto University, Kumamoto 860-0811, Japan; †Chinese Academy of Sciences Key Laboratory of Pathogenic Microbiology and Immunology, Institute of Microbiology, Chinese Academy of Sciences, Beijing 100101, People's Republic of China; ‡AIDS Clinical Center, National Center for Global Health and Medicine, Tokyo 162-8655, Japan; and §INSERM, Unité Mixte de Recherche 1135, Sorbonne Universités, Université Pierre et Marie Curie, Université Paris 06, Centre d'Immunologie et des Maladies Infectieuses-Paris, 75013, Paris, France

[1]X.S., M.F., and Y.S. contributed equally to this work.

Received for publication February 10, 2014. Accepted for publication April 28, 2014.

This work was supported by the Global Centers of Excellence program "Global Education and Research Center Aiming at the Control of AIDS," launched as a project commissioned by the Ministry of Education, Science, Sports, and Culture, Japan. This work was also supported by grants-in-aid for AIDS research from the Ministry of Health, Labour, and Welfare as well as by China National Grand Science and Technology Special Project Grant 2012ZX10001006 and by National Natural Science Foundation of China Grant 31030030.

Address correspondence and reprint requests to Prof. Masafumi Takiguchi, Center for AIDS Research, Kumamoto University, 2-2-1 Honjo, Chuo-ku, Kumamoto 860-0811, Japan. E-mail address: masafumi@kumamoto-u.ac.jp

The online version of this article contains supplemental material.

Abbreviations used in this article: MFI, mean fluorescence intensity; MHCI, MHC class I; tet, tetramer.

www.jimmunol.org/cgi/doi/10.4049/jimmunol.1400375

was obtained from all individuals according to the Declaration of Helsinki. Twenty-three HLA-A*24:02$^+$ treatment-naive individuals chronically infected with HIV-1 and eight HLA-A*24:02$^+$ HIV-1 seronegative individuals were recruited (Supplemental Table I). Their plasma and PBMCs were separated from whole blood. HLA types were determined by standard sequence-based genotyping.

HIV-1–specific CTL clones

Ag-specific CTL clones were generated as previously described (17). Briefly, RW8- and RF10-specific CTL cell lines were first obtained by stimulating PBMCs from patient KI-158 with cognate peptides. Peptide-specific CTL clones were then generated from the cell lines by limiting dilution in 96-well U-shaped plates cocultured with 1×10^6 irradiated feeder PBMCs from healthy donors and 1×10^5 irradiated C1R-A*2402 cells prepulsed with RW8 or RF10 peptide at 1 μM concentration. All CTL clones were cultured in 200 μl cloning medium (RPMI 1640 containing 10% FBS, 200 U/ml rIL-2, and 2.5% PHA soup) and stimulated weekly with irradiated C1R-A*2402 cells prepulsed with RW8 or RF10 peptide.

Tetramer staining

HLA-A*24:02 tetrameric complexes were synthesized as previously described (19). For tetramer-binding assays, CTL clones were stained with PE-conjugated RW8 or RF10 tetramers at various concentrations (0–1000 nM) at 37°C for 30 min before staining with FITC-conjugated anti-CD8 mAb at 4°C for 30 min. The cells were analyzed by using a FACSCanto II flow cytometer (BD Biosciences, San Jose, CA) and FlowJo software (Tree Star). For TCR avidity measurements, the tetramer concentration that yielded the EC_{50} mean fluorescence intensity (MFI) was calculated by probit analysis.

Cell line

C1R-A*2402 and RMA-S-A*2402 cells were previously generated by transfecting *HLA-A*24:02* genes into C1R cells and RMA-S cells, respectively (5, 20, 21). The C1R cell line is a human B cell lymphoblastoid line lacking surface expression of HLA-A and partially HLA-B molecules. It was derived from a normal B cell line, Hmy2, through three rounds of mutagenesis and selection with anti-HLA mAb (22). RMA-S cells are a TAP2 deficiency cell line derived from RMA cells. They express high levels of empty MHC molecules (i.e., not carrying endogenous peptides on the cell surface) when cultured at 26°C and very low levels when cultured at 37°C (23). RMA-S-A*2402 and C1R-A*2402 cells were cultured in RPMI 1640 medium containing 10% FCS and 0.2 mg/ml hygromycin B.

Peptide-binding assay

The binding of peptides to HLA-A*24:02 molecules was tested as previously described (24). Briefly, RMA-S-A*2402 cells were precultured at 26°C for 14–18 h and then incubated at the same temperature for 1 h with either RW8 or RF10 peptide at various concentrations (0–100 nM). Thereafter, they were incubated at 37°C for 3 h. After incubation, the peptide-pulsed cells were stained with anti-HLA class I α3 domain mAb TP25.99 (19) and subsequently with FITC-conjugated sheep IgG (Jackson ImmunoResearch Laboratories, West Grove, PA). The MFI was measured by flow cytometry (FACSCanto II).

Replication suppression assay

Two HIV-1 virus laboratory strains, NL-432-10F and NL-M20A-10F, were used in these assays. They were generated from NL-43 or NL-M20A by site-directed mutagenesis to carry the RYPLTFGWCF sequence (17). The ability of HIV-1–specific CTLs to suppress HIV-1 replication was examined as previously described (17). Briefly, primary CD4$^+$ T cells were infected with NL-432-10F and NL-M20A-10F, respectively, for 6 h before being washed with R10 medium. The cells were then cocultured with HIV-1–specific CTL clones at various E:T ratios. Ten microliters of culture supernatant was collected at day 6, and the concentration of p24 Ag in it was determined by performing p24 ELISA (ZeptMetrix, Buffalo, NY).

^{51}Cr-release assay

The cytotoxic potential of CTL clones against C1R-A*2402 prepulsed with appropriate peptide at various concentrations (0–100 nM) was determined as previously described (25). Briefly, C1R-A*2402 cells were labeled with 100 μl ^{51}Cr for 1 h before washing and then pulsed for 1 h with peptides. Effector cells were cocultured for 4 h at 37°C with target cells (2×10^3/well) at an E:T ratio of 2:1. After centrifugation, 100 μl supernatant was collected and analyzed with a gamma counter. The specific lysis was calculated as [(cpm experiment − cpm supernatant)/(cpm maximum − cpm supernatant)] × 100.

Ex vivo single-cell TCR repertoire analysis and assessment of TCR diversity

Cryopreserved PBMC samples from patients were thawed, divided, and immediately stained with RW8 or RF10 tetramers, followed by staining with anti-CD3 mAb (Pacific Blue), anti-CD8 mAb (FITC), and 7-amino-actinomycin D. RW8 and RF10 tetramer$^+$CD3$^+$CD8$^+$7-aminoactinomycin D$^-$ cells were sorted into a 96-well plates (Bio-Rad) by using a FACSAria I (BD Biosciences). Unbiased identification of TCR α- and β-chain usage was assessed as previously described (26). An Illustra ExoStar (GE Healthcare, Little Chalfont, U.K.), which contains alkaline phosphatase and exonuclease 1, was used to remove unincorporated primers and nucleotides from amplification reaction for the subsequent tailing reaction. The names of all identified TCR genes were given based on the international ImMunoGeneTics information system nomenclature (27). The diversity of TCR clonotypes was calculated by using both the number of different clonotypes and Simpson's diversity index for both α- and β-chains and the formula $D_s = 1 - \Sigma\{[n_i(n_i - 1)]/[N(N - 1)]\}$, where n_i is the TCR clone size of the ith clonotype and N is the total number of TCR sequences sampled. This index uses the relative frequency of each clonotype to calculate a diversity index ranging between 0 and 1, with 0 being minimal and 1 being maximal diversity (28).

Crystallization, data collection, and processing

Soluble peptide–HLA-A*24:02 complexes were prepared as previously described (29). HLA-A*24:02 molecules were purified by Superdex 200 10/300 GL gel-filtration chromatography (GE Healthcare). All crystallization attempts were performed by the hanging drop vapor diffusion method at 18°C with a protein/reservoir drop ratio of 1:1. Crystals were seen after 3–5 d in 0.1 M MES (pH 6.5) and 12% (w/v) polyethylene glycol at 20,000 g/mol. The crystals were briefly soaked in reservoir solution containing 17% (v/v) glycerol, mounted on an x-ray machine with a nylon loop, and then flash-cooled in a stream of gaseous nitrogen. Diffraction data were collected by using beamline NE3A in the KEK Synchrotron Facility (Tsukuba, Japan) and an ADSC Q270 imaging-plate detector at a wavelength of 1.0 Å. Data were indexed, integrated, and scaled by using HKL2000. The data collection statistics are shown in Table I. Data were analyzed by molecular replacement by use of Phaser in CCP4. We used the A24VYG molecule as the search model (Protein Data Bank accession no. 2BCK, http://www.rcsb.org/pdb/home/home.do). All of the structures were further refined by several rounds of refinement made by using the PHENIX program. The refinement statistics are given in Table I.

Results

*Effective induction of RW8- or RF10-specific CTL responses in HIV-1–infected HLA-A*24:02$^+$ patients*

To assess the degree of overlap between CTL responses specific for two superimposed Nef epitopes (RW8 and RF10), we first generated HLA-A*24:02 tetramers with RW8 or RF10 peptides (RW8-tet and RF10-tet, respectively) and compared ex vivo frequencies of 8-mer– or 10-mer–specific CD8$^+$ T cells in 23 treatment-naive HLA-A*24:02$^+$ individuals with chronic HIV-1 infection. In eight HIV-1 seronegative HLA-A*2402$^+$ donors, the frequencies of RW8 and RF10 tetramer$^+$ CD8$^+$ T cells were 0.080 ± 0.009 and 0.045 ± 0.022% (mean ± SD), respectively (Fig. 1A). We evaluated the mean ± 3 SD as positive staining and therefore considered 0.10 and 0.11% of tetramer$^+$ CD8+ cells as positive values for RW8-specific and RF10-specific T cells, respectively (Fig. 1B, dashed line). Among the 23 HIV-1–infected individuals studied, 14 and 19 were positive for RW8-specific CTLs and RF10-specific CTLs, respectively (Fig. 1A). Thirteen of the 23 individuals analyzed (56.5%) presented both RW8- and RF10-specific T cells (Fig. 1B). The magnitude of RW8-specific and RF10-specific T cells correlated with one another across individuals (Fig. 1B). However, this correlation was modest, indicating that these populations did not overlap entirely. In fact, the frequency of RF10 tetramer$^+$ CD8$^+$ cells was significantly higher than that of RW8 tetramer$^+$ CD8$^+$ cells (Fig. 1A). Taken together, these results indicate that both RW8-specific and RF10-specific CTLs could be effectively elicited in HLA-A*24:02$^+$ individuals with a chronic HIV-1 infection; however,

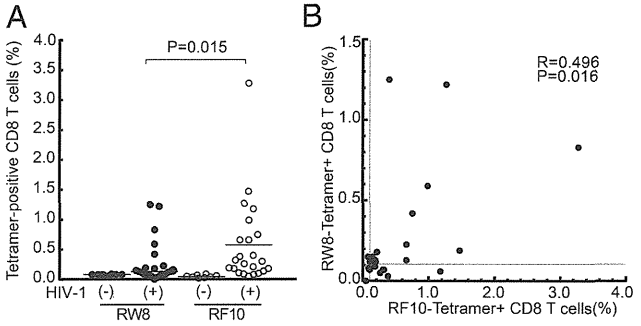

FIGURE 1. Frequencies of RW8- and RF10-specific $CD8^+$ T cells in individuals with chronic HIV-1 infection. (**A**) Frequencies of total RW8 and RF10 $tetramer^+$ $CD8^+$ T cells in 23 chronically HIV-1–infected treatment-naive HLA-A*24:02^+ individuals and in 8 HLA-A*24:02^+ uninfected controls. Statistical analyses were conducted by using the nonparametric Mann–Whitney *U* test. (**B**) Correlations between RW8 and RF10 $tetramer^+$ $CD8^+$ T cell frequencies in HIV-1–infected HLA-A*24:02^+ individuals. Of $tetramer^+$ $CD8^+$ cells, 0.10 and 0.11% were considered as positive values for RW8-specific and RF10-specific T cells, respectively (the dashed line indicates the threshold), as described in the text. The correlation was determined by using the Spearman rank test.

they do not appear to be equivalent, which begs the question of their cross-reactive potential.

Distinct reactivity of RW8- and RF10-specific CTLs

To investigate whether RW8- or RF10-specific CTLs could cross-recognize the superimposed epitopes, we first performed concurrent RW8 and RF10 tetramer (RW8-tet and RF10-tet, respectively) staining of PBMCs from HIV-1–infected donors. In patients presenting both RF10- and RW8-specific $CD8^+$ T cells, these cells did not seem to be RW8 and RF10 cross-reactive, as they failed to stain for both tetramers simultaneously. A representative case (patient KI-158) is shown in Fig. 2A. To analyze further the fine reactivity toward these epitopes, we next established CTL clones from patient KI-158 presenting both RF10- and RW8-specific $CD8^+$ T cells upon initial selection and stimulation with RW8 or RF10 peptides. RF10- and RW8-specific clones were clearly discriminated by using both tetramers together at the same concentration (Fig. 2B). We performed staining using different concentrations of the specific tetramers to measure the TCR avidity of representative RF10- or RW8-specific clones. CTL52 clone (RW8-specific) exhibited a strong affinity for RW8-tet but not for RF10-tet, whereas the CTL173 (RF10-specific) clone exhibited a strong affinity for RF10-tet but not RW8-tet (Fig. 2C), indicating that CTL52 and CTL173 clones had TCRs with high affinity for RW8 peptide–HLA-A*24:02 and RF10 peptide–HLA-A*24:02 complexes, respectively.

Next, we tested the functional avidity of RF10- and RW8-specific clones. RF10-specific clones (CTL170 and CTL173) effectively killed RF10 peptide–pulsed cells but failed to kill RW8 peptide–pulsed targets even at a high concentration of RW8 peptide (Fig. 2D), indicating that these RF10-specific clones did not cross-recognize the 8-mer peptide. RW8-specific clones (CTL52 and CTL72) recognized both RW8 peptide– and RF10 peptide–pulsed targets, but the cytotoxic activity of these clones against RW8 peptide–pulsed target cells was 10- to 50-fold higher than that against the RF10 peptide–pulsed ones (Fig. 2E). Although RW8 clones presented some cross-reactivity toward RF10, they recognized the RW8 peptide with greater efficiency than RF10. Altogether, these results indicate that RW8-specific and RF10-specific CTLs displayed no or poor cross-reactivity for their respective superimposed epitopes.

Different TCR usage between RW8- and RF10-specific $CD8^+$ T cells

The lack of cross-reactivity between RW8-specific and RF10-specific $CD8^+$ T cells implies that distinct clonotypes should

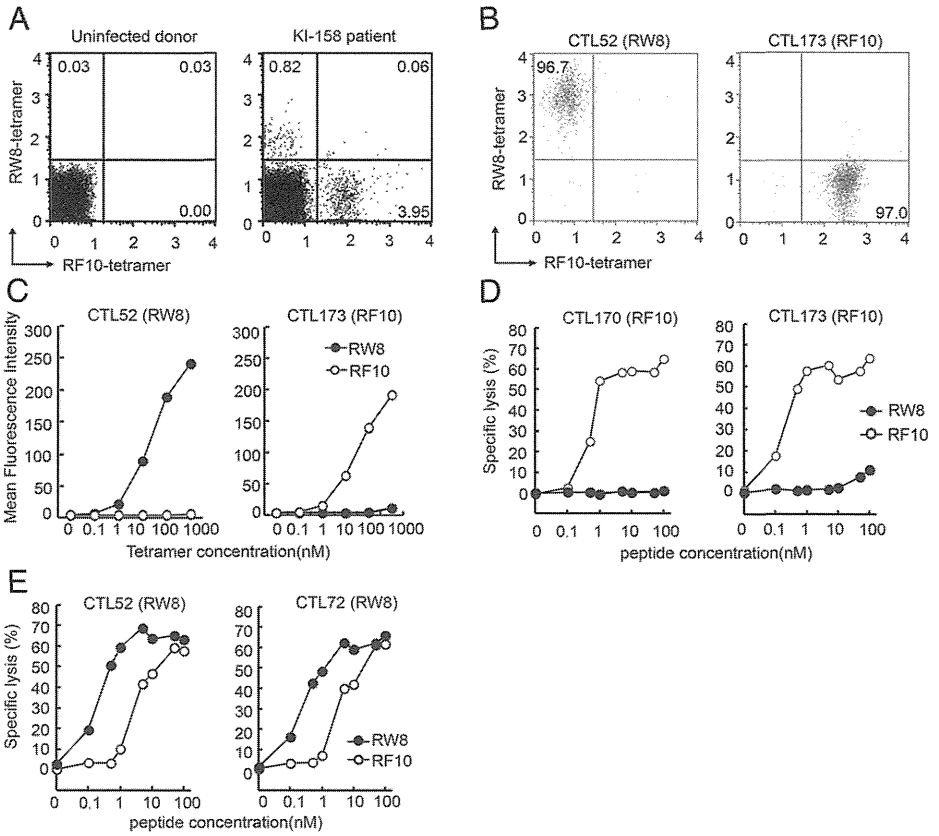

FIGURE 2. Recognition of RW8 and RF10 peptides by RW8- or RF10-specific CTL clones. (**A**) Simultaneous RW8 and RF10 tetramer staining of PBMCs from a representative HIV-1–infected donor and an HIV-1–uninfected healthy individual. The percentage of $tetramer^+$ cells among $CD8^+$ cells is shown. (**B**) Simultaneous RW8 and RF10 tetramer staining of CTL52 and CTL173 clones. The percentage of $tetramer^+$ cells among $CD8^+$ cells is shown. (**C**) RW8 and RF10 tetramer staining of CTL52 and CTL173 clones at various concentrations. Tetramer binding to CTL52 and CTL173 clones was analyzed by flow cytometry, and the data are shown as MFI. (**D** and **E**) Cytolytic activities of HLA-A*24:02–restricted RF10 (CTL170/CTL173)-specific (D) and RW8 (CTL52/CTL72)-specific (E) CTL clones toward HLA-A*24:02^+ target cells (C1R-A*2402) prepulsed with the indicated peptide at various concentrations.

comprise these populations. To verify this point, we performed TCR repertoire analysis at the single-cell level to expose the degree of overlap between the two responses at the clonotypic level. Most previous studies on TCR repertoires in virus infection or tumor studies focused mainly on characterization of the TRB gene (30–32). However, analysis of TRB genes provides only a partial account of the TCR repertoire, because the same TRB gene can pair with different TRA genes (26, 33). In the present study, we sequenced both α- and β-chains of the TCR on RW8-specific and RF10-specific single $CD8^+$ T cells sorted by FACS from three patients presenting both RW8- and RF10-specific $CD8^+$ T cells, as well as from two individuals with either one (Supplemental Table II). This analysis showed that RW8- and RF10-specific $CD8^+$ T cells consisted indeed of entirely distinct sets of clonotypes (Fig. 3, Supplemental Fig. 1). Of note, TRBV7-9 clonotypes were often detected among RW8-specific T cells, whereas TRBV28-1 was frequently found among RF10-specific T cells. Additionally, we observed that the number of distinct clonotypes as well as clonotypic diversity (based on both α- and β-chains) among RW8-specific $CD8^+$ T cells was significantly lower than for RF10-specific ones (Fig. 4). Overall, the differences in α- and β-chain TCR gene usage and overall clonotypic diversity between RW8- and RF10-specific $CD8^+$ T cells supported significantly distinct modes of TCR recognition of the RW8 peptide– and RF10 peptide–HLA-A*24:02 molecule complexes.

*Structure of RW8 peptide– and RF10 peptide–HLA-A*24:02 molecular complexes*

Considering the potential impact of peptide–MHCI structural constraints on TCR repertoire composition, we next aimed at investigating the molecular basis of the interaction between the HLA-A*24:02 molecule and the RW8 or RF10 peptide to elucidate the determining factor for the lack of overlap between RW8- and RF10-specific $CD8^+$ T cell populations. We therefore determined the crystal structure of HLA-A*24:02 in complex with RW8 (HLA-A*24:02-RW8) and HLA-A*24:02-RF10 complex (HLA-A*24:02-RF10) (Table I). The two superimposed epitopes, RF10 and RW8, showed dramatically different conformations when bound to HLA-

A Paired T cell receptor usage of RW8-specific CTLs

Sample	TRAV	TRAJ	CDR3α	TRBV	TRBD	TRBJ	CDR3β	Frequency
KI-026	TRAV12-2*03	TRAJ40*01	CAVPRTGTYKYIF	TRBV7-9*03	TRBD2*01	TRBJ2-2*01	CASSLTSGANTGELFF	10/18
	TRAV12-2*03	TRAJ23*01	CAVSFYNQGGKLIF	TRBV7-9*03	TRBD1*01	TRBJ1-2*01	CASSPRDKPNYGYTF	8/18
KI-158	TRDV1*01	TRAJ40*01	CALGELGAPGTYKYIF	TRBV20-1*01	TRBD2*01	TRBJ2-7*01	CSARDPVSTYEQYF	27/31
	TRAV12-2*02	TRAJ50*01	CAAFKTSYDKVIF	TRBV20-1*02	TRBD2*01	TRBJ2-7*01	CSARDPIRLISYEQYF	4/31
KI-654	TRAV8-4*03	TRAJ30*01	CAVSDEVIF	TRBV7-9*07	TRBD1*01	TRBJ2-5*01	CASSIRDRVPETQYF	13/43
	TRAV9-2*01	TRAJ16*01	CALFLDGQKLLF	TRBV7-9*07	TRBD2*01	TRBJ2-2*01	CASSDTSGANTGELFF	7/43
	TRAV12-2*02	TRAJ40*01	CAVPVPGTYKYIF	TRBV7-9*07	TRBD2*01	TRBJ2-2*01	CASSDTSGANTGELFF	23/43
KI-102	TRAV8-1*01	TRAJ10*01	CAVIFTGGGNKLTF	TRBV7-9*03	TRBD1*01	TRBJ2-5*01	CASSQRDSQETQYF	65/65

B Paired T cell receptor usage of RF10-specific CTLs

Sample	TRAV	TRAJ	CDR3α	TRBV	TRBD	TRBJ	CDR3β	Frequency
KI-026	TRAV9-2*01	TRAJ21*01	CALGVDFNKFYF	TRBV19*01	TRBD1*01	TRBJ2-2*01	CASKGTVTGELFF	7/27
	TRDV1*01	TRAJ9*01	CALGELTNTGGFKTIF	TRBV11-2*03	TRBD2*01	TRBJ2-7*01	CASSYDRGYEQYF	6/27
	TRDV1*01	TRAJ9*01	CALGELSRTGGFKTIF	TRBV28*01	TRBD2*02	TRBJ2-7*01	CASLPSVGKGAYEQYF	6/27
	TRDV1*01	TRAJ24*02	CALWIMTTDSWGKLQF	TRBV4-1*01	TRBD1*01	TRBJ2-1*01	CASSQSPGQGVGEQFF	4/27
	TRDV1*01	TRAJ13*02	CALGELSSGGYQKVTF	TRBV6-1*01	TRBD1*01	TRBJ1-2*01	CASSDVGQGSSNYGYTF	2/27
	TRDV1*01	TRAJ36*01	CALGVLDQTGANNLFF	TRBV28*01	TRBD1*01	TRBJ1-2*01	CASSSPGQGYGYTF	1/27
	TRAV21*02	TRAJ7*01	CAVWYYGNNRLAF	TRBV28*01	TRBD2*02	TRBJ2-2*01	CASSLMGLAGVPGELF	1/27
KI-158	TRDV1*01	TRAJ9*01	CALGELSGTGGFKTIF	TRBV6-1*01	TRBD1*01	TRBJ2-1*01	CASSEGFGQGGIEQFF	19/32
	TRDV1*01	TRAJ53*01	CALGELLRGGSNYKLTF	TRBV6-2*01	TRBD2*01	TRBJ2-7*01	CASSYSHRLGLHEQYF	11/32
	TRAV8-6*02	TRAJ48*01	CAVLSLISNFGNEKLTF	TRBV19*01	TRBD2*01	TRBJ2-7*01	CASSISAGEGVPEQYF	2/32
KI-118	TRDV1*01	TRAJ9*01	CALGELSSTGGFKTIF	TRBV28*01	TRBD1*01	TRBJ2-1*01	CASTSFGQGTNEQFF	12/14
	TRAV13-1*02	TRAJ20*01	CAALNDYKLSF	TRBV19*01	TRBD2*01	TRBJ2-1*01	CASSIDPPGLADNEQFF	2/14
KI-102	TRDV1*01	TRAJ9*01	CALGELSHTGGFKTIF	TRBV11-2*01	TRBD1*01	TRBJ2-7*01	CASSYDRSYEQYF	4/30
	TRDV1*01	TRAJ9*01	CALGELTNTGGFKTIF	TRBV6-6*01	TRBD1*01	TRBJ1-2*01	CASSYSIGTGVNNYGYTF	3/30
	TRDV1*01	TRAJ36*01	CALGVLDQTGANNLFF	TRBV28*01	TRBD1*01	TRBJ1-2*01	CASSSPGQGYGYTF	7/30
	TRDV1*01	TRAJ54*01	CALGVIGIQGAQKLVF	TRBV28*01	TRBD1*01	TRBJ1-5*01	CASSPSTGKGNQPQHF	7/30
	TRAV25*01	TRAJ23*01	CPFYNQGGKLIF	TRBV19*01	TRBD1*01	TRBJ1-2*01	CASSTALRTGNYGYTF	4/30
	TRAV26-1*01	TRAJ28*01	CVVNSGAGSYQLTF	TRBV6-1*01	TRBD1*01	TRBJ2-7*01	CASSETGGTYEQYF	3/30
	TRAV8-3*02	TRAJ37*01	CAVDEGKLIF	TRBV4-1*01	TRBD1*01	TRBJ1-1*01	CASSQRDRGTDTEAFF	1/30
	TRAV14/DV4*01	TRAJ33*01	CAMQDSNYQLIW	TRBV7-9*03	TRBD2*02	TRBJ2-1*01	CASSLVSGRGNEQFF	1/30

FIGURE 3. Clonotypic analysis of RW8- and RF10-specific $CD8^+$ T cells. Single RW8- or RF10-specific $CD8^+$ T cells from five chronically HIV-1–infected HLA-A*24:02^+ individuals were FACS sorted, and TCR α- and β-chain sequencing was performed. Paired TCR α- and β-chain usage, CDR3 amino acid sequences, and individual clonotype frequencies are shown. (**A**) Paired T cell receptor usage of RW8-specific CTLs. (**B**) Paired T cell receptor usage of RF10-specific CTLs.

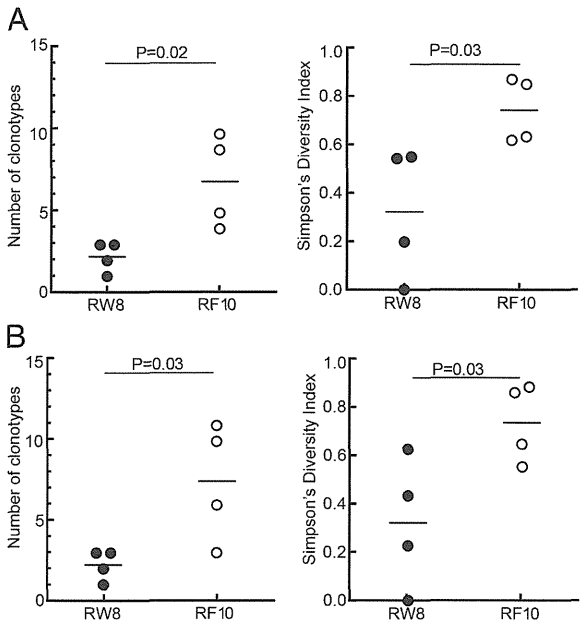

FIGURE 4. TCR repertoire diversity of RW8- and RF10-specific $CD8^+$ T cells. TCR repertoire diversity was assessed by using both the number of clonotypes and Simpson's diversity index for α- (**A**) and β-chain (**B**). Statistical analysis was conducted by use of the unpaired *t* test.

A*24:02 (Fig. 5A). The RW8 peptide was buried in the binding groove. In contrast, the two extra amino acids at the C terminus of the RF10 peptide caused a switch of the Pc anchor residues from Trp^8 in RW8 to Phe^{10} in RF10, so that the central region (P4–P7) of RF10 protruded out of the groove. Therefore, the solvent-accessible surface area of the central region of RF10 significantly diverged from that of RW8. These dramatic conformational differences explain the lack of cross-reactivity between RW8- and RF10-specific CTLs, as well as the necessity to elicit different TCR repertoires to recognize these HLA-A*24:02 superimposed epitopes.

The total hydrogen bonds and van der Waal's interactions between HLA-A*24:02 and the RW8 or RF10 peptide were analyzed in detail (Fig. 5B, Supplemental Table III). The first 3 aa (P1–P3 residues) of both RW8 and RF10 peptides displayed almost identical main-chain conformations. However, the N-terminal anchor residue (Pn) tyrosine (Y) at position P2 formed a hydrogen bond with H70 in the B pocket of HLA-A*24:02. One additional hydrogen bond between P2 residue and Lys^{66} and another hydrogen bond between the P1 residue and Arg^{170} were also observed in the RF10 peptide. Moreover, whereas the Pc residue Trp^8 of the RW8 peptide formed four hydrogen bonds with the HLA molecule, the subanchor residue Trp^8 and Pc residue Phe^{10} of the RF10 peptide formed one more hydrogen bond. This additional hydrogen bonding likely impacted the binding affinity of RF10 for HLA-A*24:02, making it greater than that of RW8.

Superior HIV-suppressive capacity of RF10-specific $CD8^+$ CTL clones

Measurements of the binding affinity of RF10 and RW8 peptides for HLA-A*24:02 molecules indeed revealed that the RF10 affinity was ~10-fold higher than the RW8 affinity (Fig. 6A). Such differences in peptide–MHCI binding affinity may eventually have affected the efficiency of T cells to recognize their specific targets. We thus investigated the ability of RW8- and RF10-specific $CD8^+$ CTL clones to suppress HIV-1 replication in cultures of virus-infected $CD4^+$ T lymphocytes. To this end, we used two viruses, NL-432-10F and NL-M20A-10F, both carrying the RYPLTFGWCF sequence. In contrast to NL-432-10F, NL-M20A-10F does not downregulate cell-surface expression of HLA class I molecules (34). A previous study demonstrated the epitope-dependent effect of Nef-mediated HLA class I downregulation on the capacity of HIV-1 specific CTLs to suppress HIV-1 replication. The capacity may be dependent on the expression level of HLAI molecules

Table I. Statistics for crystallographic data collection and structure refinement

	A24, 8-Mer	A24, 10-Mer
Data collection		
Space group	$P2_1$	C2
Cell dimensions		
a, *b*, *c* (Å)	71.95, 152.52, 90.17	161.74, 65.06, 50.42
α, β, γ (°)	90.00, 90.12, 90.00	90.00, 90.23, 90.00
Resolution (Å)	50.0–2.4	50.0–2.4
R_{merge}	0.087 (0.554)[a]	0.102 (0.469)
$I/\sigma I$	13.0 (2.2)	20.0 (2.6)
Completeness (%)	99.3 (99.3)	97.2 (92.6)
Redundancy	3.1 (3.1)	4.1 (3.6)
Refinement		
Resolution (Å)	36.0–2.4	42.7–2.4
No. of reflections	70,383	20,284
R_{work}/R_{free}	0.1952/0.2185	0.1882/0.2223
No. of atoms		
Protein	12,528	3,148
Water	609	238
B factors		
Protein	46.5	38.4
Water	38.0	40.0
R.m.s.d.		
Bond lengths (Å)	0.004	0.003
Bond angles (°)	0.857	0.689
Ramachandran plot (%)		
Most favored regions	87.9	96.3
Allowed regions	12.1	3.7
Disallowed regions	0	0

[a]Values in parentheses are for the highest resolution shell.
R.m.s.d., root mean square deviations.

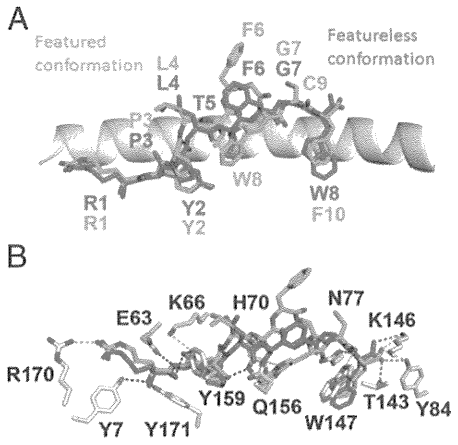

FIGURE 5. Comparison between the structure of the HLA-A24:02 molecule in complex with the RW8 or RF10 epitope peptide. (**A**) Superposition of HLA-A*24:02 in complex with RW8 (pink) or RF10 (green) peptides. The peptides are shown in stick-model form. RF10 displays a featured conformation with the residue F6 exposed to the solvent, whereas RW8 displays a featureless conformation, with the residue F6 hidden in the groove. (**B**) Hydrogen bond interactions between HLA-A*24:02 and RW8 (pink) or RF10 (green) peptide. The hydrogen bonds in common between the two peptides are shown in black.

carrying the epitope peptide (35). RF10-specific CTL clones 170 and 173 completely suppressed the replication of both NL-432-10F and NL-M20A-10F at E:T ratios of 1:1 and 0.1:1, respectively, indicating that RF10-specific CTLs could strongly suppress HIV-1 replication regardless of Nef-mediated downregulation of HLA class I molecules (Fig. 6B). In comparison, the ability of RW8-specific CTL clones 52 and 72 to suppress NL-432-10F was weaker than that of RF10-specific CTLs, even at an E:T ratio of 1:1, although their respective capacities to suppress NL-M20A-10F were comparable (Fig. 6B). These results indicate that RF10-specific CTLs presented higher Ag sensitivity than did RW8-specific CTLs, implying that the RF10 peptide is more presented on the cell surface than is the RW8 peptide.

In addition to the higher binding affinity of HLA-A*24:02 for the RF10 peptide, we wanted to compare the TCR avidity of RW8- and RF10-specific $CD8^+$ T cell clones. We thus measured TCR avidity of these clones by using the tetramer dilution assay. Twelve clones of each specificity were stained with different concentrations of RW8-tet or RF10-tet (Fig. 6C). The EC_{50} values of the RF10-specific CTL clones were significantly lower than those of the RW8-specific ones (Fig. 6D), indicating that RF10-specific $CD8^+$ T cells had a higher TCR avidity than did the RW8-specific $CD8^+$ T cells.

Discussion

Screening for optimal CTL epitopes is central for the characterization of antiviral or antitumoral $CD8^+$ T cell responses (36–38). It is not unusual to observe CTL reactivity toward peptides of 8–12 aa in length around an optimal epitope. This observation is thought to reflect the flexibility of TCR–MHC pairing to accommodate peptides close to the optimal one, such that the same $CD8^+$ T cells are able to recognize these peptides (39–41). In the present study, we examined $CD8^+$ T cell responses against two superimposed HIV nef epitopes (RW8 and RF10) restricted by HLA-A*24:02. Using RW8 and RF10 tetramers, we could discriminate between T cells specific for these two peptides and could show that these cells represented two distinct populations with independent reactivity. Furthermore, we applied single-cell TCR analysis to characterize both TCR α- and β-chain repertoires directly

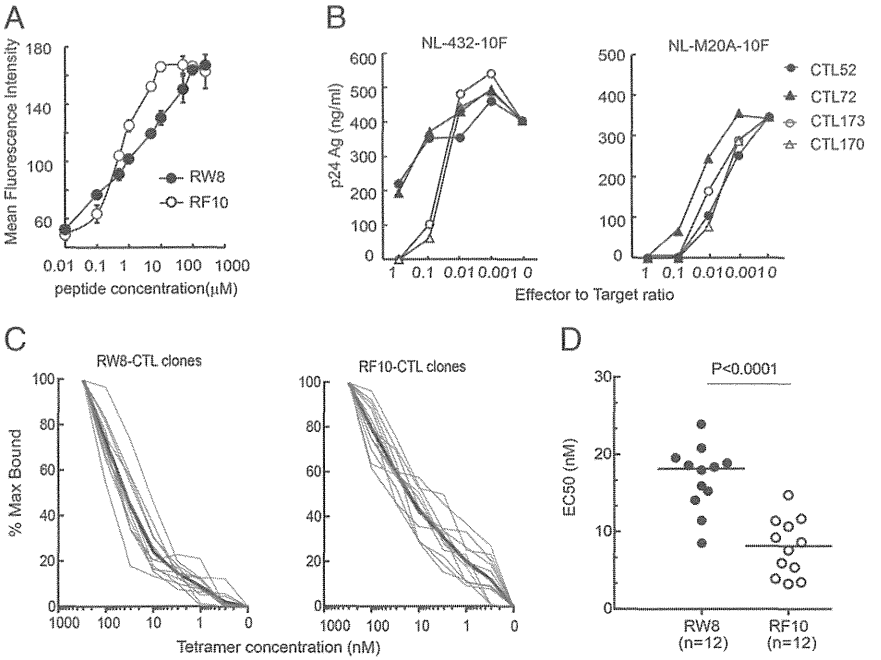

FIGURE 6. Efficacy of superimposed epitope-specific CTLs to suppress HIV-1 replication. (**A**) Binding of RW8 and RF10 peptides to HLA-A*24:02 molecules on RMA-S-A*2402 cells quantified by use of the HLA-A*24:02 stabilization assay. (**B**) HIV suppressive capacity of two RW8-specific CTL clones (CTL 52 and 72) and two RF10-specific CTL clones (CTL 170 and 173). Cultured $CD4^+$ T cells derived from an HLA-A*24:02^+ donor were infected with NL-432-10F or NL-M20A-10F and then cocultured with the indicated CTL clones at various E:T ratios. HIV-1 p24 Ags in the supernatant were measured on day 6 postinfection by performing an enzyme immunoassay. (**C**) Normalized MFI of staining with specific tetramers at concentrations from 0.3 to 300 nM for RF10- and RW8-specific CTL clones was used to calculate TCR avidity. Individual clones (gray lines) and the mean value of each group (black line) are shown. (**D**) TCR avidity of RF10- and RW8-specific CTL clones. The EC_{50} of tetramer staining (MFI) was calculated for each clone from (C). The statistical comparison was conducted by using the nonparametric Mann–Whitney *U* test.

from cryopreserved PBMCs and could show that different TCR repertoires were elicited as responses against the two superimposed epitopes. RW8 and RF10 epitopes presented by HIV-1–infected cells are therefore recognized by independent specific T cells. Thus, RYPLTFGWCF (RF10) presented two epitopes to HLA-A*24:02, with each eliciting a distinct CTL response. We analyzed in the present study the ability of CTL clones from a single individual to recognize these epitopes and to suppress HIV-1. Additional analyses using CTL clones from other individuals would be useful to confirm the conclusion of the present study.

Previous studies indicated that HLA-B57–restricted KI8 and KF10 or HLA-B35–restricted VY8 and RY11 superimposed epitopes induce independent CTL responses (7, 10), but that HLA-B54–restricted FV9 and FP10 superimposed epitopes elicit mainly cross-reactive CTLs in HIV-1–infected patients (8). Although the detailed mechanisms remain unclear, these studies suggest that different lengths or conformations of a peptide may determine the nature of the CTL response. Our comprehensive analysis of RW8-specific and RF10-specific $CD8^+$ T cells, showing no overlap or cross-reactivity between these two populations, is in line with a recent report that peptide length determines the outcome of TCR/peptide–MHCI engagement (42). This study shows indeed that a given TCR is predisposed to engage peptides of a defined length so that TCR plasticity and cross-reactivity are strictly restricted to a single MHCI–peptide length.

Emerging evidence also indicates that conformational features of peptides presented in the groove of HLA molecules can partially determine the diversity of the TCR repertoire (43), although consensus is still lacking. It was reported that epitopes with featured conformations are associated with a highly diverse TCR repertoire (44–46) and that a featureless epitope results in the generation a less diverse TCR repertoire (47). However, the opposite result was also reported, with a featureless epitope (HCMV pp65, FPTKDVAL) being associated with diverse TCR usage (48). In the present study, we examined two immunodominant superimposed epitopes, derived from the same antigenic source and restricted through the same MHC allele, and we used unbiased single-cell *TRA* and *TRB* sequence analyses to compare TCR α- and β-chain repertoire diversity in the same individuals. Compared to previous studies, the present one was therefore particularly appropriate for investigating the effect of epitope conformation on TCR repertoire diversity. Our data showed that featured (RF10) and featureless (RW8) epitope conformations were indeed associated with a diverse and restricted TCR repertoire, respectively, in line with the putative availability of clonotypes in the naive T cell pool able to recognize the epitopes.

A diverse TCR repertoire is thought to facilitate the selection of CTLs with high avidity and therefore to influence their functional properties and efficacy against viruses (49–53). We indeed found that the binding affinity of specific tetramers for RF10-specific CTL clones was significantly higher than that for RW8-specific ones, suggesting that the former CTLs had higher TCR avidity than did the latter ones. Moreover, RF10-specific clones presented a stronger ability to suppress HIV-1 in vitro than did RW8-specific clones, and the frequency of RF10-specific CTLs was higher than that of RW8-specific CTLs in HIV-1–infected individuals. Taken together, our data support the idea that the selection of high-avidity TCRs is associated with TCR repertoire diversity and suggest that RF10-specific CTLs exert a superior control of HIV-1 replication in vivo compared with RW8-specific CTLs.

In conclusion, we investigated HLA-A*24:02–restricted CTLs specific for superimposed Nef epitopes, RF10 and RW8, by using multiple approaches. We demonstrated that RW8 and RF10 peptides bound to HLA-A*24:02, resulting in different peptide conformations. This difference was responsible for the induction of totally different CTL responses, that is, no cross-reactivity, distinct TCR repertoires, and different functional avidity. Our study provides a clear demonstration that superimposed epitopes restricted by the same HLA molecule could elicit entirely different $CD8^+$ T cell responses. We show that this difference was linked to featured versus featureless epitope conformations, yielding distinct TCR repertoires for the two CTL populations. The featured RF10 epitope was associated with the induction of T cells carrying TCRs with high diversity and avidity. This finding is directly relevant to our understanding of $CD8^+$ T cell–mediated control of HIV-1, as well as to the choice of immunogens for vaccine design. Our findings indicate that targeting a single viral sequence, for example, RF10, can lead to the induction of two immune responses against HIV and thus enhance the suppression of its replication.

Acknowledgments

We thank Sachiko Sakai for secretarial assistance.

Disclosures

The authors have no financial conflicts of interest.

References

1. Rammensee, H. G., K. Falk, and O. Rötzschke. 1993. Peptides naturally presented by MHC class I molecules. *Annu. Rev. Immunol.* 11: 213–244.
2. Yewdell, J. W., E. Reits, and J. Neefjes. 2003. Making sense of mass destruction: quantitating MHC class I antigen presentation. *Nat. Rev. Immunol.* 3: 952–961.
3. Garcia, K. C., L. Teyton, and I. A. Wilson. 1999. Structural basis of T cell recognition. *Annu. Rev. Immunol.* 17: 369–397.
4. Choppin, J., W. Cohen, A. Bianco, J. P. Briand, F. Connan, M. Dalod, and J. G. Guillet. 2001. Characteristics of HIV-1 Nef regions containing multiple $CD8^+$ T cell epitopes: wealth of HLA-binding motifs and sensitivity to proteasome degradation. *J. Immunol.* 166: 6164–6169.
5. Ikeda-Moore, Y., H. Tomiyama, K. Miwa, S. Oka, A. Iwamoto, Y. Kaneko, and M. Takiguchi. 1997. Identification and characterization of multiple HLA-A24-restricted HIV-1 CTL epitopes: strong epitopes are derived from V regions of HIV-1. *J. Immunol.* 159: 6242–6252.
6. Le Gall, S., P. Stamegna, and B. D. Walker. 2007. Portable flanking sequences modulate CTL epitope processing. *J. Clin. Invest.* 117: 3563–3575.
7. Goulder, P. J., Y. Tang, S. I. Pelton, and B. D. Walker. 2000. HLA-B57-restricted cytotoxic T-lymphocyte activity in a single infected subject toward two optimal epitopes, one of which is entirely contained within the other. *J. Virol.* 74: 5291–5299.
8. Hashimoto, M., T. Akahoshi, H. Murakoshi, N. Ishizuka, S. Oka, and M. Takiguchi. 2012. CTL recognition of HIV-1-infected cells via cross-recognition of multiple overlapping peptides from a single 11-mer Pol sequence. *Eur. J. Immunol.* 42: 2621–2631.
9. Stewart-Jones, G. B., G. Gillespie, I. M. Overton, R. Kaul, P. Roche, A. J. McMichael, S. Rowland-Jones, and E. Y. Jones. 2005. Structures of three HIV-1 HLA-B*5703-peptide complexes and identification of related HLAs potentially associated with long-term nonprogression. *J. Immunol.* 175: 2459–2468.
10. Ueno, T., C. Motozono, S. Dohki, P. Mwimanzi, S. Rauch, O. T. Fackler, S. Oka, and M. Takiguchi. 2008. CTL-mediated selective pressure influences dynamic evolution and pathogenic functions of HIV-1 Nef. *J. Immunol.* 180: 1107–1116.
11. Saito, S., S. Ota, E. Yamada, H. Inoko, and M. Ota. 2000. Allele frequencies and haplotypic associations defined by allelic DNA typing at HLA class I and class II loci in the Japanese population. *Tissue Antigens* 56: 522–529.
12. Naruto, T., H. Gatanaga, G. Nelson, K. Sakai, M. Carrington, S. Oka, and M. Takiguchi. 2012. HLA class I-mediated control of HIV-1 in the Japanese population, in which the protective HLA-B*57 and HLA-B*27 alleles are absent. *J. Virol.* 86: 10870–10872.
13. Chikata, T., J. M. Carlson, Y. Tamura, M. A. Borghan, T. Naruto, M. Hashimoto, H. Murakoshi, A. Q. Le, S. Mallal, M. John, et al. 2014. Host-specific adaptation of HIV-1 subtype B in the Japanese population. *J. Virol.* 88: 4764–4775.
14. Sobao, Y., K. Sugi, H. Tomiyama, S. Saito, S. Fujiyama, M. Morimoto, S. Hasuike, H. Tsubouchi, K. Tanaka, and M. Takiguch. 2001. Identification of hepatitis B virus-specific CTL epitopes presented by HLA-A*2402, the most common HLA class I allele in East Asia. *J. Hepatol.* 34: 922–929.
15. Nakamoto, Y., S. Kaneko, H. Takizawa, Y. Kikumoto, M. Takano, Y. Himeda, and K. Kobayashi. 2003. Analysis of the CD8-positive T cell response in Japanese patients with chronic hepatitis C using HLA-A*2402 peptide tetramers. *J. Med. Virol.* 70: 51–61.
16. Tanuma, J., M. Fujiwara, K. Teruya, S. Matsuoka, H. Yamanaka, H. Gatanaga, N. Tachikawa, Y. Kikuchi, M. Takiguchi, and S. Oka. 2008. HLA-A*2402-restricted HIV-1-specific cytotoxic T lymphocytes and escape mutation after ART with structured treatment interruptions. *Microbes Infect.* 10: 689–698.

17. Fujiwara, M., J. Tanuma, H. Koizumi, Y. Kawashima, K. Honda, S. Mastuoka-Aizawa, S. Dohki, S. Oka, and M. Takiguchi. 2008. Different abilities of escape mutant-specific cytotoxic T cells to suppress replication of escape mutant and wild-type human immunodeficiency virus type 1 in new hosts. *J. Virol.* 82: 138–147.
18. Goulder, P. J., A. Edwards, R. E. Phillips, and A. J. McMichael. 1997. Identification of a novel HLA-A24-restricted cytotoxic T-lymphocyte epitope within HIV-1 Nef. *AIDS* 11: 1883–1884.
19. Tanabe, M., M. Sekimata, S. Ferrone, and M. Takiguchi. 1992. Structural and functional analysis of monomorphic determinants recognized by monoclonal antibodies reacting with the HLA class I alpha 3 domain. *J. Immunol.* 148: 3202–3209.
20. Karaki, S., A. Kariyone, N. Kato, K. Kano, Y. Iwakura, and M. Takiguchi. 1993. HLA-B51 transgenic mice as recipients for production of polymorphic HLA-A, B-specific antibodies. *Immunogenetics* 37: 139–142.
21. Takamiya, Y., C. Schönbach, K. Nokihara, M. Yamaguchi, S. Ferrone, K. Kano, K. Egawa, and M. Takiguchi. 1994. HLA-B*3501-peptide interactions: role of anchor residues of peptides in their binding to HLA-B*3501 molecules. *Int. Immunol.* 6: 255–261.
22. Zemmour, J., A. M. Little, D. J. Schendel, and P. Parham. 1992. The HLA-A,B "negative" mutant cell line C1R expresses a novel HLA-B35 allele, which also has a point mutation in the translation initiation codon. *J. Immunol.* 148: 1941–1948.
23. Ljunggren, H. G., N. J. Stam, C. Ohlén, J. J. Neefjes, P. Höglund, M. T. Heemels, J. Bastin, T. N. Schumacher, A. Townsend, K. Kärre, et al. 1990. Empty MHC class I molecules come out in the cold. *Nature* 346: 476–480.
24. Ibe, M., Y. I. Moore, K. Miwa, Y. Kaneko, S. Yokota, and M. Takiguchi. 1996. Role of strong anchor residues in the effective binding of 10-mer and 11-mer peptides to HLA-A*2402 molecules. *Immunogenetics* 44: 233–241.
25. Fujiwara, M., and M. Takiguchi. 2007. HIV-1-specific CTLs effectively suppress replication of HIV-1 in HIV-1-infected macrophages. *Blood* 109: 4832–4838.
26. Sun, X., M. Saito, Y. Sato, T. Chikata, T. Naruto, T. Ozawa, E. Kobayashi, H. Kishi, A. Muraguchi, and M. Takiguchi. 2012. Unbiased analysis of TCRα/β chains at the single-cell level in human CD8+ T-cell subsets. *PLoS ONE* 7: e40386.doi:10.1371/journal.pone.0040386
27. Lefranc, M. P., V. Giudicelli, C. Ginestoux, J. Jabado-Michaloud, G. Folch, F. Bellahcene, Y. Wu, E. Gemrot, X. Brochet, J. Lane, et al. 2009. IMGT, the international ImMunoGeneTics information system. *Nucleic Acids Res.* 37(Database issue): D1006–D1012.
28. Venturi, V., K. Kedzierska, S. J. Turner, P. C. Doherty, and M. P. Davenport. 2007. Methods for comparing the diversity of samples of the T cell receptor repertoire. *J. Immunol. Methods* 321: 182–195.
29. Shi, Y., J. Qi, A. Iwamoto, and G. F. Gao. 2011. Plasticity of human CD8αα binding to peptide-HLA-A*2402. *Mol. Immunol.* 48: 2198–2202.
30. Almeida, J. R., D. A. Price, L. Papagno, Z. A. Arkoub, D. Sauce, E. Bornstein, T. E. Asher, A. Samri, A. Schnuriger, I. Theodorou, et al. 2007. Superior control of HIV-1 replication by $CD8^+$ T cells is reflected by their avidity, polyfunctionality, and clonal turnover. *J. Exp. Med.* 204: 2473–2485.
31. Robins, H. S., P. V. Campregher, S. K. Srivastava, A. Wacher, C. J. Turtle, O. Kahsai, S. R. Riddell, E. H. Warren, and C. S. Carlson. 2009. Comprehensive assessment of T-cell receptor β-chain diversity in αβ T cells. *Blood* 114: 4099–4107.
32. van Bockel, D. J., D. A. Price, M. L. Munier, V. Venturi, T. E. Asher, K. Ladell, H. Y. Greenaway, J. Zaunders, D. C. Douek, D. A. Cooper, et al. 2011. Persistent survival of prevalent clonotypes within an immunodominant HIV gag-specific $CD8^+$ T cell response. *J. Immunol.* 186: 359–371.
33. Dash, P., J. L. McClaren, T. H. Oguin, III, W. Rothwell, B. Todd, M. Y. Morris, J. Becksfort, C. Reynolds, S. A. Brown, P. C. Doherty, and P. G. Thomas. 2011. Paired analysis of TCRα and TCRβ chains at the single-cell level in mice. *J. Clin. Invest.* 121: 288–295.
34. Akari, H., S. Arold, T. Fukumori, T. Okazaki, K. Strebel, and A. Adachi. 2000. Nef-induced major histocompatibility complex class I down-regulation is functionally dissociated from its virion incorporation, enhancement of viral infectivity, and CD4 down-regulation. *J. Virol.* 74: 2907–2912.
35. Tomiyama, H., M. Fujiwara, S. Oka, and M. Takiguchi. 2005. Cutting edge: epitope-dependent effect of Nef-mediated HLA class I down-regulation on ability of HIV-1-specific CTLs to suppress HIV-1 replication. *J. Immunol.* 174: 36–40.
36. Ladell, K., M. Hashimoto, M. C. Iglesias, P. G. Wilmann, J. E. McLaren, S. Gras, T. Chikata, N. Kuse, S. Fastenackels, E. Gostick, et al. 2013. A molecular basis for the control of preimmune escape variants by HIV-specific $CD8^+$ T cells. *Immunity* 38: 425–436.
37. Gross, D. A., S. Graff-Dubois, P. Opolon, S. Cornet, P. Alves, A. Bennaceur-Griscelli, O. Faure, P. Guillaume, H. Firat, S. Chouaib, et al. 2004. High vaccination efficiency of low-affinity epitopes in antitumor immunotherapy. *J. Clin. Invest.* 113: 425–433.
38. Ciernik, I. F., J. A. Berzofsky, and D. P. Carbone. 1996. Induction of cytotoxic T lymphocytes and antitumor immunity with DNA vaccines expressing single T cell epitopes. *J. Immunol.* 156: 2369–2375.
39. Rudolph, M. G., R. L. Stanfield, and I. A. Wilson. 2006. How TCRs bind MHCs, peptides, and coreceptors. *Annu. Rev. Immunol.* 24: 419–466.
40. Willcox, B. E., G. F. Gao, J. R. Wyer, J. E. Ladbury, J. I. Bell, B. K. Jakobsen, and P. A. van der Merwe. 1999. TCR binding to peptide-MHC stabilizes a flexible recognition interface. *Immunity* 10: 357–365.
41. Baker, B. M., D. R. Scott, S. J. Blevins, and W. F. Hawse. 2012. Structural and dynamic control of T-cell receptor specificity, cross-reactivity, and binding mechanism. *Immunol. Rev.* 250: 10–31.
42. Ekeruche-Makinde, J., J. J. Miles, H. A. van den Berg, A. Skowera, D. K. Cole, G. Dolton, A. J. Schauenburg, M. P. Tan, J. M. Pentier, S. Llewellyn-Lacey, et al. 2013. Peptide length determines the outcome of TCR/peptide-MHCI engagement. *Blood* 121: 1112–1123.
43. Turner, S. J., P. C. Doherty, J. McCluskey, and J. Rossjohn. 2006. Structural determinants of T-cell receptor bias in immunity. *Nat. Rev. Immunol.* 6: 883–894.
44. Kjer-Nielsen, L., C. S. Clements, A. W. Purcell, A. G. Brooks, J. C. Whisstock, S. R. Burrows, J. McCluskey, and J. Rossjohn. 2003. A structural basis for the selection of dominant αβ T cell receptors in antiviral immunity. *Immunity* 18: 53–64.
45. Tynan, F. E., H. H. Reid, L. Kjer-Nielsen, J. J. Miles, M. C. Wilce, L. Kostenko, N. A. Borg, N. A. Williamson, T. Beddoe, A. W. Purcell, et al. 2007. A T cell receptor flattens a bulged antigenic peptide presented by a major histocompatibility complex class I molecule. *Nat. Immunol.* 8: 268–276.
46. Stewart-Jones, G. B., A. J. McMichael, J. I. Bell, D. I. Stuart, and E. Y. Jones. 2003. A structural basis for immunodominant human T cell receptor recognition. *Nat. Immunol.* 4: 657–663.
47. Turner, S. J., K. Kedzierska, H. Komodromou, N. L. La Gruta, M. A. Dunstone, A. I. Webb, R. Webby, H. Walden, W. Xie, J. McCluskey, et al. 2005. Lack of prominent peptide-major histocompatibility complex features limits repertoire diversity in virus-specific $CD8^+$ T cell populations. *Nat. Immunol.* 6: 382–389.
48. Wynn, K. K., Z. Fulton, L. Cooper, S. L. Silins, S. Gras, J. K. Archbold, F. E. Tynan, J. J. Miles, J. McCluskey, S. R. Burrows, et al. 2008. Impact of clonal competition for peptide-MHC complexes on the $CD8^+$ T-cell repertoire selection in a persistent viral infection. *Blood* 111: 4283–4292.
49. Cornberg, M., A. T. Chen, L. A. Wilkinson, M. A. Brehm, S. K. Kim, C. Calcagno, D. Ghersi, R. Puzone, F. Celada, R. M. Welsh, and L. K. Selin. 2006. Narrowed TCR repertoire and viral escape as a consequence of heterologous immunity. *J. Clin. Invest.* 116: 1443–1456.
50. Meyer-Olson, D., N. H. Shoukry, K. W. Brady, H. Kim, D. P. Olson, K. Hartman, A. K. Shintani, C. M. Walker, and S. A. Kalams. 2004. Limited T cell receptor diversity of HCV-specific T cell responses is associated with CTL escape. *J. Exp. Med.* 200: 307–319.
51. Kedzierska, K., N. L. La Gruta, M. P. Davenport, S. J. Turner, and P. C. Doherty. 2005. Contribution of T cell receptor affinity to overall avidity for virus-specific $CD8^+$ T cell responses. *Proc. Natl. Acad. Sci. USA* 102: 11432–11437.
52. Messaoudi, I., J. A. Guevara Patiño, R. Dyall, J. LeMaoult, and J. Nikolich-Zugich. 2002. Direct link between mhc polymorphism, T cell avidity, and diversity in immune defense. *Science* 298: 1797–1800.
53. Appay, V., D. C. Douek, and D. A. Price. 2008. $CD8^+$ T cell efficacy in vaccination and disease. *Nat. Med.* 14: 623–628.

TCR repertoire usage for RW8-specific CTLs

Sample	Va	Ja	CDR3	Frequency	Sample	Vb	Db	Jb	CDR3	Frequency
KI-026	TRAV12-2*03	TRAJ40*01	CAVPRTGTYKYIF	16/29	KI-026	TRBV7-9*03	TRBD2*01	TRBJ2-2*01	CASSLTSGANTGELFF	14/30
	TRAV12-2*03	TRAJ23*01	CAVSFYNQGGKLIF	12/29		TRBV7-9*03	TRBD1*01	TRBJ1-2*01	CASSPRDKPNYGYTF	12/30
	TRAV5*01	TRAJ4*01	CAETLPGGGYNKLIF	1/29		TRBV11-3*01	TRBD1*01	TRBJ2-2*01	CASSLAVRGLSGDPFF	4/30
KI-158	TRDV1*01	TRAJ40*01	CALGELGAPGTYKYIF	33/37	KI-158	TRBV20-1*01	TRBD2*01	TRBJ2-7*01	CSARDPVSTYEQYF	43/49
	TRAV12-2*02	TRAJ50*01	CAAFKTSYDKVIF	4/37		TRBV20-1*02	TRBD2*01	TRBJ2-7*01	CSARDPIRLISYEQYF	4/49
KI-654	TRAV8-4*03	TRAJ30*01	CAVSDEVIF	13/43		TRBV3-1*01	TRBD1*01	TRBJ2-7*01	CASSQPTGREQYF	2/49
	TRAV9-2*01	TRAJ16*01	CALFLDGQKLLF	7/43	KI-654	TRBV7-9*07	TRBD1*01	TRBJ2-5*01	CASSIRDRVPETQYF	20/65
	TRAV12-2*02	TRAJ40*01	CAVPVPGTYKYIF	23/43		TRBV7-9*07	TRBD2*01	TRBJ2-2*01	CASSDTSGANTGELFF	45/65
KI-102	TRAV8-1*01	TRAJ10*01	CAVIFTGGGNKLTF	65/65	KI-102	TRBV7-9*03	TRBD1*01	TRBJ2-5*01	CASSQRDSQETQYF	86/86

TCR repertoire usage for RF10-specific CTLs

KI-026	TRAV9-2*01	TRAJ21*01	CALGVDFNKFYF	10/34	KI-026	TRBV19*01	TRBD1*01	TRBJ2-2*01	CASKGTVTGELFF	12/44
	TRDV1*01	TRAJ9*01	CALGELTNTGGFKTIF	6/34		TRBV11-2*03	TRBD2*01	TRBJ2-7*01	CASSYDRGYEQYF	9/44
	TRDV1*01	TRAJ9*01	CALGELSRTGGFKTIF	6/34		TRBV28*01	TRBD2*02	TRBJ2-7*01	CASLPSVGKGAYEQYF	6/44
	TRDV1*01	TRAJ24*02	CALWIMTTDSWGKLQF	4/34		TRBV4-1*01	TRBD1*01	TRBJ2-1*01	CASSQSPGQGVGEQFF	4/44
	TRAV40*01	TRAJ32*02	CFLGSYGGATTKLIF	3/34		TRBV28*01	TRBD2*01	TRBJ2-2*01	CASSLRPGRANTGELFF	3/44
	TRDV1*01	TRAJ13*02	CALGELSSGGYQKVTF	2/34		TRBV3-1*01	TRBD1*01	TRBJ1-1*01	CASSSLGQGAPEAFF	3/44
	TRDV1*01	TRAJ36*01	CALGVLDQTGANNLFF	1/34		TRBV6-1*01	TRBD1*01	TRBJ2-3*01	CASSDFSKGTDTQYF	3/44
	TRAV21*02	TRAJ7*01	CAVWYYGNNRLAF	1/34		TRBV6-1*01	TRBD1*01	TRBJ1-2*01	CASSDVGQGSSNYGYTF	2/44
	TRAV17*01	TRAJ15*01	CATDAKAGTALIF	1/34		TRBV28*01	TRBD1*01	TRBJ1-2*01	CASSSPGQGYGYTF	1/44
KI-158	TRDV1*01	TRAJ9*01	CALGELSGTGGFKTIF	22/37		TRBV28*01	TRBD2*02	TRBJ2-2*01	CASSLMGLAGVPGELF	1/44
	TRDV1*01	TRAJ53*01	CALGELLRGGSNYKLTF	11/37	KI-158	TRBV6-1*01	TRBD1*01	TRBJ2-1*01	CASSEGFGQGGIEQFF	31/48
	TRAV8-6*02	TRAJ48*01	CAVLSLISNFGNEKLTF	2/37		TRBV6-2*01	TRBD2*01	TRBJ2-7*01	CASSYSHRLGLHEQYF	15/48
	TRAV8-6*02	TRAJ39*01	CAVSCLRNNAGNMLTF	2/37		TRBV19*01	TRBD2*01	TRBJ2-7*01	CASSISAGEGVPEQYF	2/48
KI-118	TRDV1*01	TRAJ9*01	CALGELSSTGGFKTIF	15/21	KI-118	TRBV28*01	TRBD1*01	TRBJ2-1*01	CASTSFGQGTNEQFF	16/25
	TRAV13-1*02	TRAJ20*01	CAALNDYKLSF	3/21		TRBV19*01	TRBD2*01	TRBJ2-1*01	CASSIDPPGLADNEQFF	3/25
	TRAV21*02	TRAJ37*02	CAVFSSNTGKLIF	1/21		TRBV7-9*03	TRBD1*01	TRBJ2-2*01	CASSPGSGELGAGELFF	2/25
	TRAV26-1*01	TRAJ42*01	CIVYGGSQGNLIF	1/21		TRBV23-1*01	TRBD1*01	TRBJ1-5*01	CASSQSRQGAQPQHF	1/25
	TRAV6*02	TRAJ13*02	CALLGISGGYQKVTF	1/21		TRBV11-2*01	TRBD1*01	TRBJ2-7*01	CASSLGRDRPTPYEQYF	1/25
KI-102	TRDV1*01	TRAJ54*01	CALGVIGIQGAQKLVF	9/38		TRBV27*01	TRBD1*01	TRBJ2-1*01	CASTTSNEQFF	2/25
	TRDV1*01	TRAJ36*01	CALGVLDQTGANNLFF	8/38	KI-102	TRBV28*01	TRBD1*01	TRBJ1-2*01	CASSSPGQGYGYTF	10/41
	TRAV26-1*01	TRAJ28*01	CVVNSGAGSYQLTF	5/38		TRBV28*01	TRBD1*01	TRBJ1-5*01	CASSPSTGKGNQPQHF	7/41
	TRDV1*01	TRAJ9*01	CALGELSHTGGFKTIF	4/38		TRBV19*01	TRBD1*01	TRBJ1-2*01	CASSTALRTGNYGYTF	6/41
	TRDV1*01	TRAJ9*01	CALGELTNTGGFKTIF	4/38		TRBV11-2*01	TRBD1*01	TRBJ2-7*01	CASSYDRSYEQYF	4/41
	TRAV25*01	TRAJ23*01	CPFYNQGGKLIF	4/38		TRBV6-6*01	TRBD1*01	TRBJ1-2*01	CASSYSIGTGVNNYGYTF	3/41
	TRAV8-3*02	TRAJ37*01	CAVDEGKLIF	1/38		TRBV4-1*01	TRBD2*01	TRBJ2-7*01	CASSPVAGVYEQYF	3/41
	TRAV14/DV4*01	TRAJ33*01	CAMQDSNYQLIW	1/38		TRBV28*01	TRBD2*01	TRBJ2-1*01	CASSLESLGLASVDEQFF	2/41
	TRAV13-2*01	TRAJ10*01	CAEVSTGGGNKLTF	1/38		TRBV25-1*01	TRBD1*01	TRBJ2-5*01	CASSAPRETQYF	2/41
	TRAV17*01	TRAJ15*01	CATDWQAGTALIF	1/38		TRBV6-1*01	TRBD1*01	TRBJ2-7*01	CASSETGGTYEQYF	2/41
						TRBV4-1*01	TRBD1*01	TRBJ1-1*01	CASSQRDRGTDTEAFF	1/41
						TRBV7-9*03	TRBD2*02	TRBJ2-1*01	CASSLVSGRGNEQFF	1/41

Figure S1. Clonotypic analysis of RW8- and RF10-specific CD8+ T cells

Supplemental Table I. Information of participants in this study

ID	HLA						VL	CD4	Date
	A allele		B allele		C allele		(copies/ml)	(cells/μl)	(M/D/Y)
U[a]-4	1101	**2402**	5201	5201	1202	1402			
U-13	0201	**2402**	5101	6701	0702	1402			
U-14	0201	**2402**	3501	5401	0102	0303			
U-15	**2402**	**2402**	1501	5401	0102	0801			
U-23	**2402**	3303	4403	5101	nt[b]				
U-24	0201	**2402**	5201	5901	nt				
U-35	0201	**2402**	3501	5201	0303	1202			
U-36	0201	**2402**	3901	5201	nt				
KI[c]-021	**2402**	2602	5101	6701	0702	1402	<50	578	11/02/04
KI-026	0206	**2402**	4006	5101	0801	1402	40000	526	07/07/05
KI-042	**24**	31	35	60	03	07	4800	441	01/20/00
KI-060	**2402**	2601	4002	5201	1202	0304	13000	533	08/30/03
KI-067	**2402**	**2402**	4801	5201	1202	1202	89000	234	01/25/00
KI-068	**2402**	3303	0702	4403	nt		15000	346	12/13/01
KI-069	**2402**	**2402**	4006	5201	0304	1202	19000	263	11/16/99
KI-071	**2402**	3101	4006	5201	nt		48000	292	01/25/00
KI-092	0206	**2402**	4801	5101	0801	1402	220	971	08/14/03
KI-102	0206	**2402**	0702	3501	0303	0702	13000	355	03/28/05
KI-108	**2402**	**2402**	5201	5201	1202	1202	2100	469	12/18/03
KI-113	**2402**	**2402**	0701	5201	0702	1202	31000	192	07/24/01
KI-116	**2402**	**2402**	1501	5201	0303	1202	250000	156	12/13/01
KI-117	0201	**2402**	1301	4801	nt		180000	151	07/31/01
KI-118	**2402**	3101	3902	4403	0702	1403	240	279	07/31/01
KI-123	**2402**	2601	1501	1518	0704	0801	66000	406	08/20/02
KI-127	0206	**2402**	4002	5101	nt		9300	519	10/20/05
KI-130	**2402**	**2402**	0702	5201	0702	1202	14000	351	10/02/01
KI-133	**2402**	**2402**	4006	4403	0801	1403	5500	664	12/18/03
KI-148	1102	**2402**	2704	2711	1202	1502	13000	647	02/08/02
KI-158	**2402**	3303	5201	4403	1202	1403	200	611	10/10/03
KI-188	**2402**	**2402**	1501	4403	0303	1403	630	360	08/05/04
KI-194	0201	**2402**	5201	5201	1202	1202	210	672	08/20/05

U[a:] HIV-1 seronegative individual nt[b:] not test KI[c:] HIV-1 seropositive patients

Supplemental Table II. Information on patients used for TCR repertoire analysis of RW8- and RF10-specific CTLs

Patient ID	HLA-A	Median VL (copies/ml)	Median CD4 (cells/μl)	Sample date (Mo/Day/Yr)	Tetramer frequency in CD8 T cells(%)	
					RW8	RF10
KI-026[a]	A0206/A2402	$9.2x10^4$	502	01/20/2005	1.07	1.2
KI-102[b]	A0206/A2402	580	482	08/23/2002	0.91	0.72
KI-118[a]	A3101/A2402	240	279	07/31/2001	N.D[c]	0.15
KI-158[b]	A3303/A2402	160	321	05/24/2004	0.62	1.42
KI-654[a]	A6802/A2402	$1.8x10^4$	357	07/08/2009	1.23	N.D

[a]: treatment naïve [b]: STI (structured treatment interruption) patients [c]: N.D: not detected

Supplemental Table III. Hydrogen bonds and van der Waal's interactions for the HLA-A*2402-peptide complexes

	Peptide		Hydrogen bond partner		
	Residue	atom	Residue	atom	Contact residue
A24-8mer	R^{1}	N	Y^{7}	OH	M^{5}, Y^{7}, Y^{59}, E^{63}, Y^{159}, R^{170}, Y^{171} (28)[a]
	R^{1}	N	Y^{171}	OH	
	R^{1}	O	Y^{159}	OH	
	Y^{2}	N	E^{63}	OE1	Y^{7}, S^{9}, F^{22}, A^{24}, V^{27}, M^{45}, E^{63}, K^{66}, H^{70}, M^{97},
	Y^{2}	O	Y^{159}	OH	Y^{159} (38)
	Y^{2}	OH	H^{70}	ND1	
	P^{3}				Y^{7}, F^{99} (12)
	L^{4}				K^{66}, H^{114}, Q^{155}, Q^{156} (5)
	T^{5}				H^{70}, T^{73}, M^{97}, Y^{116} (11)
	F^{6}				N^{77}, W^{147}, V^{152}, Q^{156} (9)
	G^{7}				N^{77}, W^{147} (7)
	W^{8}	N	N^{77}	OD1	N^{77}, I^{80}, Y^{84}, L^{95}, Y^{116}, Y^{123}, T^{143}, K^{146}, W^{147} (64)
	W^{8}	O	Y^{84}	OH	
	W^{8}	O	T^{143}	OG1	
	W^{8}	OXT	K^{146}	NZ	
A24-10mer	R^{1}	N	Y^{7}	OH	M^{5}, Y^{7}, E^{63}, K^{66}, Y^{159}, G^{167}, R^{170}, Y^{171} (28)
	R^{1}	N	Y^{171}	OH	
	R^{1}	NH2	R^{170}	NH1	
	R^{1}	O	Y^{159}	OH	
	Y^{2}	N	E^{63}	OE1	Y^{7}, S^{9}, F^{22}, A^{24}, M^{45}, E^{63}, K^{66}, V^{67}, H^{70}, Y^{159}
	Y^{2}	O	Y^{159}	OH	(38)
	Y^{2}	O	K^{66}	NZ	
	Y^{2}	OH	H^{70}	ND1	
	P^{3}				F^{99}, Y^{159} (12)
	L^{4}				K^{66}, Q^{156}, Y^{159} (5)
	T^{5}				H^{70}, T^{73} (12)
	F^{6}				
	G^{7}				V^{152}, W^{147} (3)
	W^{8}	NE1	Q^{156}	NE2	N^{77}, M^{97}, F^{99}, H^{114}, Y^{116}, W^{147}, Q^{156} (32)
	W^{8}	O	N^{77}	ND2	
	C^{9}	O	W^{147}	NE1	N^{77}, W^{147} (7)
	F^{10}	N	N^{77}	OD1	N^{77}, I^{80}, Y^{84}, Y^{116}, Y^{123}, T^{143}, K^{146} (42)
	F^{10}	O	Y^{84}	OH	
	F^{10}	O	K^{146}	NZ	

[a]: Residues within 4 Å of peptide with total number of contacts in parentheses